



Semiannual Report

Growth, Nitrogen Vacancy Reduction and Solid Solution Formation in Cubic GaN Thin Films and the Subsequent Fabrication of Superlattice Structures Using AlN and InN

Supported under Grant #N00014-86-K-0686 P5
Innovative Science and Technology Office
of the Strategic Defense Initiative
Office of the Chief of Naval Research
Report for the period January 1, 1992-June 30, 1992

DTIC
S ELECTE D
A
JUL 28 1992

Robert F. Davis, K. Shawn Ailey-Trent, Daniel Kester,
Michael J. Paisley, Bill Perry, Laura Smith, and Cheng Wang
Materials Science and Engineering Department
North Carolina State University
Campus Box 7907
Raleigh, NC 27695-7907

This document has been approved
for public release and sale; its
distribution is unlimited.

June 1992

92-20028



REPORT DOCUMENTATION PAGE

Form Approved
OMB No 0704 0188

Public reporting burden for this collection of information is estimated to average 1 hour per response, including the time for reviewing instructions, searching existing data sources, gathering and maintaining the data needed, and completing and reviewing the collection of information. Send comments regarding this burden estimate or any aspect of this collection of information, including suggestions for reducing this burden to Washington Headquarters Services, Directorate for Information Operations and Reports, 1215 Jefferson Davis Highway, Suite 1204, Arlington, VA 22202-4302, and to the Office of Management and Budget, Paperwork Reduction Project (0704-0188), Washington, DC 20503.

1. AGENCY USE ONLY (Leave blank)	2. REPORT DATE June 1992	3. REPORT TYPE AND DATES COVERED Semiannual 1/1/92-6/30/92
----------------------------------	-----------------------------	---

4. TITLE AND SUBTITLE Growth, Nitrogen Vacancy Reduction and Solid Solution Formation in Cubic GaN Thin Films and the Subsequent Fabrication of Superlattice Structures Using AlN and InN	5. FUNDING NUMBERS R&T:s400001srq05 S.O.:1114SS
--	---

6. AUTHOR(S) Robert F. Davis	
-------------------------------------	--

7. PERFORMING ORGANIZATION NAME(S) AND ADDRESS(ES) North Carolina State University Hillsborough Street Raleigh, NC 27695	8. PERFORMING ORGANIZATION REPORT NUMBER N00014-86-K-0686 P5
---	---

9. SPONSORING / MONITORING AGENCY NAME(S) AND ADDRESS(ES) Sponsoring: ONR, 800 N. Quincy, Arlington, VA 22217 Monitoring: Office of Naval Research Resider, N66005 The Ohio State Univ. Research Center 1314 Kinnear Road Columbus, OH 43212-1194	10. SPONSORING / MONITORING AGENCY REPORT NUMBER
--	--

11. SUPPLEMENTARY NOTES

12a. DISTRIBUTION / AVAILABILITY STATEMENT Approved for Public Release—Distribution Unlimited	12b. DISTRIBUTION CODE
--	------------------------

13. ABSTRACT (Maximum 200 words)

Undoped GaN films have been deposited by gas-source MBE having essentially intrinsic electrical character. Acceptor-type behavior has been achieved with Mg doping. The electrical properties of these latter films were resistivity = 0.5 Ω·cm, Hall mobility (holes = 10 cm²/V·s and carrier concentration = 1 × 10¹⁸ cm⁻³. Photo-assisted gas-source MBE growth of stoichiometric GaN has also been achieved using a 500 W Hg lamp. Illumination and Ga cell temperature altered the texture of the polycrystalline GaN in unusual ways, changing the growth habit from (0001)∥(100) to (0001)∥(111) and back again. Thin films of cubic-BN (c-BN) have also been deposited on various substrates via both gas-source MBE and electron beam MBE. The use of Si (100) substrates, the latter technique and the characterization tools of RHEED, XPS, LEED, SEM, FTIR and HRTEM resulted in the achievement of an initial amorphous BN layer followed by a layer of turbostratic BN and subsequently by a layer of cubic BN. Cubic BN films were also deposited on polycrystalline diamond films grown via CVD on Si(100). The effect of the bombarding species was examined. Finally, the plans for both a systematic investigation of the ion implantation and contact development and related characterization of AlN and GaN with n- and p-type dopants and the construction and employment of a UV luminescence facility is discussed.

14. SUBJECT TERMS gallium nitride, aluminum nitride, boron nitride, Fourier transform infrared spectroscopy, transmission electron microscopy, photoluminescence, gas-source MBE, cathodoluminescence, ion implantation	15. NUMBER OF PAGES 58
	16. PRICE CODE

17. SECURITY CLASSIFICATION OF REPORT UNCLAS	18. SECURITY CLASSIFICATION OF THIS PAGE UNCLAS	19. SECURITY CLASSIFICATION OF ABSTRACT UNCLAS	20. LIMITATION OF ABSTRACT SAR
---	--	---	-----------------------------------

VI. Impurity Doping and Contact Formation in AlN and GaN	50
A. Introduction	50
B. Proposed Experimental Procedure	50
1. Impurity Doping of AlN and GaN	50
2. Electrical Contacts to AlN and GaN	52
C. Summary	55
D. References	55
VII. Development of Ultra-violet-Visible Luminescence Facility	56
A. Introduction	56
B. Future Research Plans/Goals	56
C. References	57
VIII. Distribution List	58

I. Introduction

Continued development and commercialization of optoelectronic devices, including light-emitting diodes and semiconductor lasers produced from III-V gallium arsenide-based materials, has also generated interest in the much wider bandgap semiconductor mononitride materials containing boron, aluminum, gallium, and indium. The majority of the studies have been conducted on pure gallium nitride thin films having the wurtzite structure, and this emphasis continues to the present day. Recent research has resulted in the fabrication of p-n junctions in both wurtzite gallium nitride and cubic boron nitride, the deposition of cubic gallium and indium nitrides, as well as the fabrication of multilayer heterostructures and the formation of thin film solid solutions. Chemical vapor deposition (CVD) has usually been the technique of choice for thin film fabrication. However, more recently these materials have also been deposited by plasma-assisted CVD, reactive ionized-cluster beam deposition and reactive and ionized molecular beam epitaxy.

The program objectives in this reporting period have been (1) the deposition via gas-source MBE of intrinsic and p-type doped GaN, (2) photo-assisted deposition of GaN, (3) the deposition of cubic BN via gas-source and electron beam MBE, (4) development plans for systematic contact and ion implantation studies of dopants in AlN and GaN and the initial research in the latter. The procedures, results, discussions of these results, conclusions and plans for future research of these studies are given in the following sections. Note that each major section is self-contained with its own figures, tables, and references.

II. Deposition of Intrinsic Undoped and P-type Mg-doped GaN Films

A. Introduction

During the last three decades, the growth and characterization of GaN film has received considerable attention [1]. However, until recently, its application in terms of devices has been relegated to mis light emitting diodes due to the unsuccessful deposition of p-type GaN films. To date, the introduction of acceptor-type dopants, such as Mg and Zn, resulted only in compensation. For example, the electrical properties of the GaN films changed from being highly conductive n-type, for the undoped film to highly resistive for the acceptor doped. However, recently a Japanese research group observed p-type character in a Mg-doped GaN film after a post-deposition Low-Energy Electron-Beam Irradiation (LEEBI) treatment [2]. However, there is no explanation for this phenomena. In order to make realistic device applications, one should have the capability to activate the acceptor dopants in GaN during growth and, thus, to make p-type GaN films directly.

B Experimental Procedures

The deposition system employed in this research was a commercial Perkin-Elmer 430 MBE system. This system consists of three parts: a load lock (base pressure of 5×10^{-8} Torr), a transfer tube (base pressure of 1×10^{-10} Torr), which also was used for degas the substrates, and the growth chamber (base pressure of 5×10^{-11} Torr). Knudson effusion cells with BN crucibles and Ta wire heaters were charged with 7N pure gallium, 6N pure aluminum and 6N pure magnesium, respectively. Ultra-high purity nitrogen, further purified by a chemical purifier, was used as the sources gas. It was excited by an ECR plasma source, which was designed to fit inside the 2.25 inch diameter tube of the source flange cryoshroud. The details of the system can be found elsewhere [3].

The substrates were (0001) oriented α (6H)-SiC and epitaxial quality sapphire wafers. Prior to loading into the chamber, the α -SiC substrates were cleaned by a standard degreasing and RCA cleaning procedures. The sapphire substrates were cleaned using the following procedure: degreasing and DI water rinse, 10 minutes in a hot solution of $\text{HPO}_3:\text{H}_2\text{SO}_4$ with 1:1 ratio, DI water rinse thoroughly, finally dip in 1:10 solution of 49% $\text{HF}:\text{H}_2\text{O}$. All substrates were then mounted on a 3-inch molybdenum block and loaded into the system. After undergoing a degassing procedure (700°C for 30 minutes), the substrates were transferred into the deposition chamber. Finally RHEED was performed to examine the crystalline quality of the substrates.

C. Results

1. Deposition of High Quality Undoped GaN Films

In the past, single crystal GaN films have been successfully deposited on a variety of substrates using the NCSU modified gas source MBE system. However, the resistivity of those as-deposited films was low and they exhibited a n-type conductive character. We have also found for the films deposited on α -SiC substrates, there was a thin amorphous silicon nitride layer at the interface of substrates and the deposited GaN films [4]. This resulted from the use of the nitrogen ECR plasma source in order to obtain reactive nitrogen species during the deposition. RHEED patterns of both the α -SiC and sapphire substrates changed after exposure to the nitrogen plasma for times as little as five minutes. These patterns showed increasingly disordered structures with an increase in the exposure time. In order to deposit good quality GaN films, this amorphous interfacial layer must be eliminated.

We have developed the following technique to prevent this amorphous interfacial layer from forming on the substrate surface. The procedure involves an initial exposure of the substrate to pure Al followed by the exposure of this Al to reactive N. During this time, the Al layers reacted with the plasma activated nitrogen species and formed an AlN layer. The details of reacting metal Al with activated N₂ species to form AlN can be found in a report by J.A. Taylor [5]. The film growth was subsequently started using the deposition conditions listed in the Table I.

Table I. Deposition Conditions for Undoped GaN Films.

Nitrogen pressure	2×10^{-4} Torr
Microwave power	50W
Gallium cell temperature	990°C
Aluminum cell temperature	1120°C
substrate temperature	650°C
Al layer	2 monatomic layer
AlN buffer layer	150~200Å
GaN	4000~5000Å

An AlN buffer layer having a thickness of about 150Å was used to reduce the lattice mismatch between the substrate and GaN [6]. Reflection High Energy Electron Diffraction (RHEED) and SEM were performed to examine the quality of the deposited GaN films. RHEED patterns taken on the $\langle 2\bar{1}10 \rangle$ azimuth of GaN films deposited on (0001)-oriented α -SiC and sapphire substrates are shown in Figure 1. An analysis of these RHEED patterns

indicated that both the AlN buffer layer and the GaN film are monocrystalline. The RHEED pattern of the final surface of the GaN films indicated that they had reasonable crystalline quality and smooth surface. Kikuchi lines were observed on the RHEED screen, but cannot be photographed due to the low contrast. A spotty RHEED pattern was obtained for the GaN film deposited on the sapphire substrates due to sample charging of the resistive film. This is also discussed below. The surface morphology of the films was also examined by SEM. The featureless picture, shown in Figure 2, is indicative of the smooth surface of the deposited GaN film and agreed well with the the RHEED pattern results.

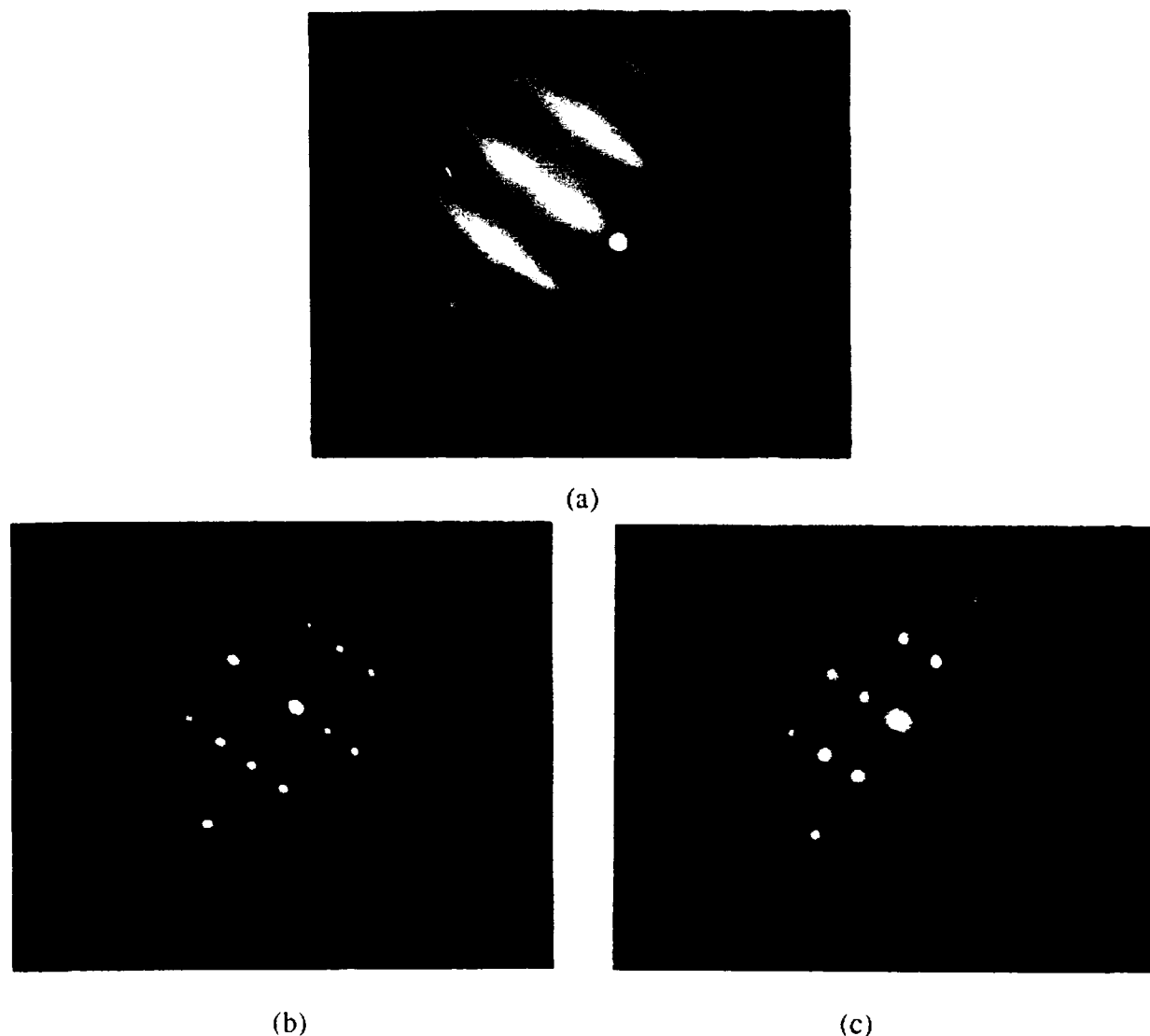


Figure 1. RHEED patterns taken in the $\langle 2\bar{1}10 \rangle$ azimuth of (a) an AlN buffer layer on a $\alpha(6H)\text{-SiC}$ substrate, (b) a GaN film on the AlN/ $\alpha(6H)\text{-SiC}$ substrate, (c) a GaN film on an AlN/sapphire substrate.

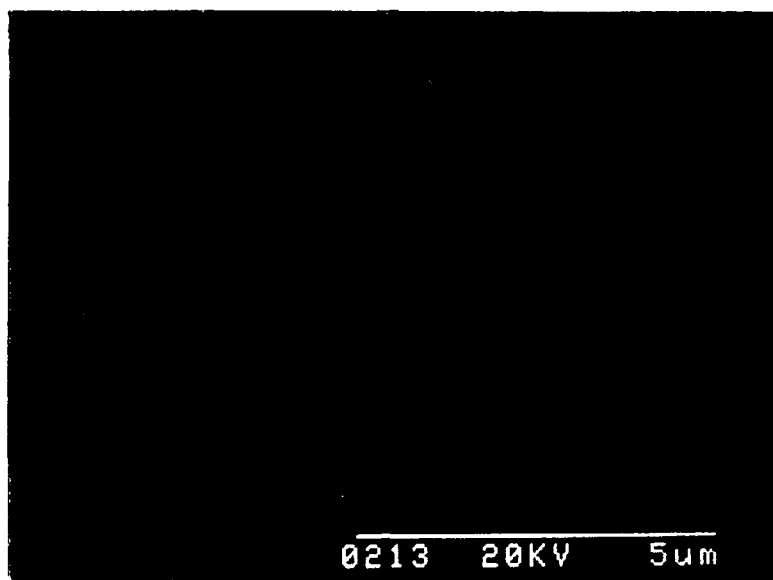


Figure 2. SEM photograph of the surface of an undoped GaN film deposited on a AlN/ α -SiC substrate.

Structural characterization and epitaxial relationships were studied by cross-section transmission electron microscopy. TEM was performed in a JEOL 4000EX operated at 350 kV. High resolution images were recorded using a 1 mrad convergence semi-angle. As shown in Figure 3, films of GaN with an AlN buffer layer grown on off-axis α (6H)-SiC(0001) and on α -Al₂O₃(0001) have been compared. In each case the films were epitaxial across the AlN/substrate and GaN/AlN interfaces. The film grown on α -Al₂O₃ showed a columnar structure, possibly due to planar defects such as low angle grain boundaries. The film grown on SiC appeared to be of better quality with respect to planar defect concentrations. The deposition on SiC resulted in a thicker AlN buffer layer and a thicker GaN layer even though both samples were grown during the same run. In order to analyze the defect structure of the films, plan view samples will be studied. In addition, more in-depth study of the AlN/substrate interface and the GaN/AlN interface is planned.

2. Deposition of Mg-doped GaN Films

Based on above results, we investigated the incorporation of the acceptor dopant, Mg, into the films. The deposition conditions for Mg-doped GaN films were same as that for undoped GaN films described above, except that a Mg-source was used in the deposition. Table II lists the typical deposition conditions for Mg-doped GaN films

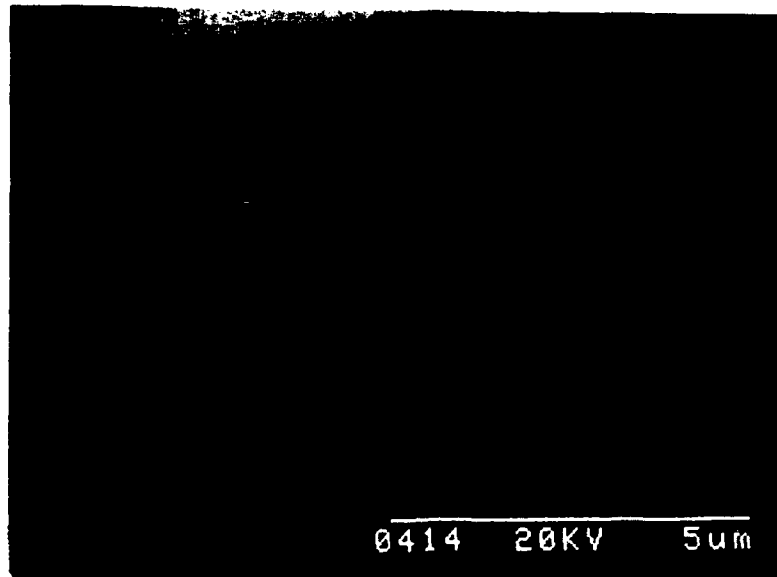


Figure 3. TEM micrographs showing a film of GaN with an AlN buffer layer grown on a) an off-axis α -SiC substrate and b) an α -Al₂O₃ substrate.

Table II. Deposition Conditions for Mg-doped GaN Films

Nitrogen pressure	2×10^{-4} Torr
Microwave power	50W
Gallium cell temperature	990°C
Aluminum cell temperature	1120°C
Magnesium cell temperature	~300°C
substrate temperature	650°C
Al layer	2 monatomic layer
AlN buffer layer	150~200Å
Mg-doped GaN	4000~5000Å

The RHEED patterns of the Mg-doped films also showed features indicative of good crystalline quality. Similar to the undoped GaN films, the representative SEM picture in Figure 4 shows that the Mg-doped GaN films also had a very smooth surface.

3. Electrical Properties of the Undoped and Mg-doped GaN Films

The electrical properties of the films have been characterized by van der Pauw resistivity measurements and Hall effect measurements. Indium was used as the electrical contacts. Current-voltage (IV) measurements were first performed to check the contact character. As shown in Fig. 5(a), the undoped GaN film was quite resistive; a non-ohmic IV character was

observed after voltage larger than 15 volts was applied. The Mg-doped GaN films were much more conductive, as shown in Figure 5(b), and IV measurements of the contacts indicated ohmic character. It is clear from this point that eliminating the amorphous interfacial layer at the substrate surface results in a dramatic improvement in the electrical properties. The early work conducted in our research group has shown that even Mg-doped GaN made at that time possessed a similar non-ohmic IV character to that of undoped GaN film made in this reporting period [7]. Resistivity and Hall effect measurements were performed for both undoped and Mg-doped GaN films. The results are summarized in Table III. Note that for the undoped GaN films, the highly resistive character made the electrical measurements very difficult. By contrast, for the Mg-doped GaN films, a p-type conductive character was identified, and the measured electrical properties were similar to those recently reported for the low-energy electron-beam irradiation (LEEBI) treated Mg-doped GaN film [2,8].

Table III. Electrical Properties of Undoped and Mg-doped GaN Films.

films	undoped GaN	Mg-doped GaN
resistivity ($\Omega\cdot\text{cm}$)	$>10^2$	0.3
conductive type	x	P-type
mobility ($\text{cm}^2/\text{V}\cdot\text{s}$)	?	~ 10
carrier concentration (cm^{-3})	$<10^{16}$	$\sim 1 \cdot 10^{18}$

The temperature dependence of the resistivity for a p-type Mg-doped GaN film has also been measured. The results are shown in Figure 6. The resistivity decrease with increasing temperature is due to the increasing ionization of the Mg acceptor dopant.

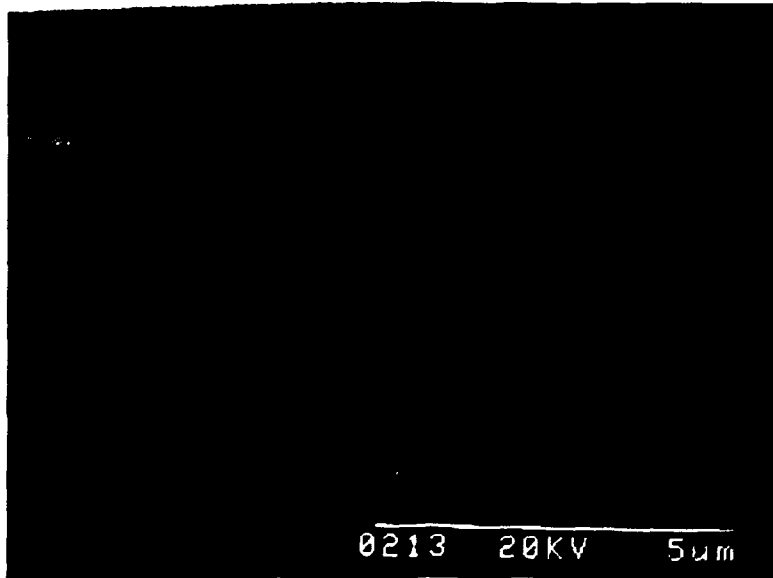


Figure 4. SEM photograph of the surface of the undoped GaN film deposited on an AlN/ α -SiC substrate.

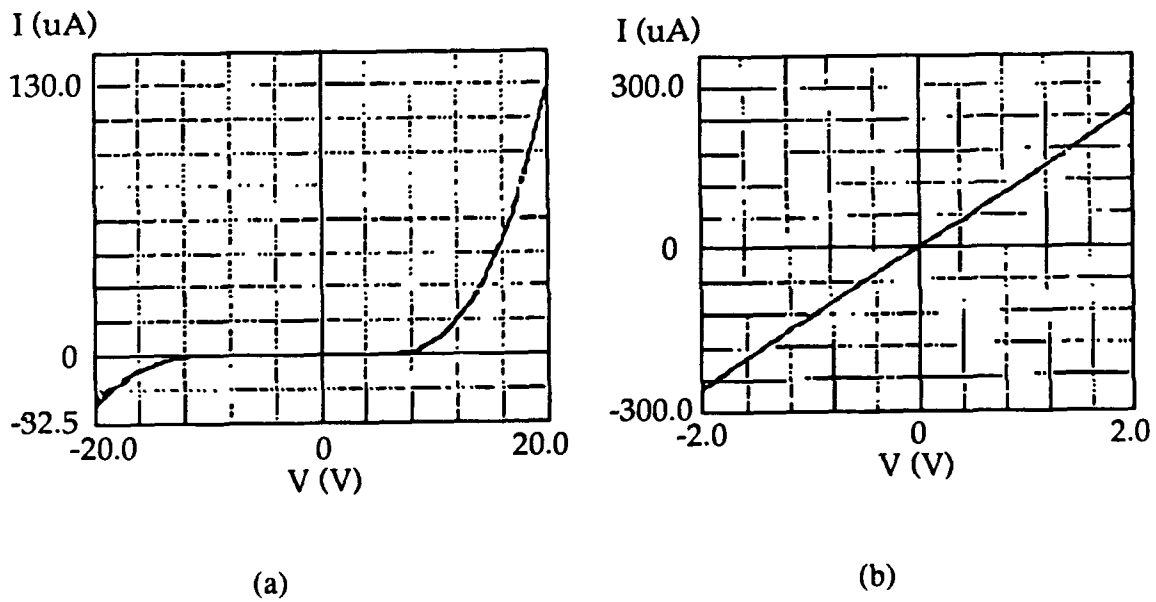


Figure 5. IV Curves for (a) an undoped GaN film, (b) a Mg-doped GaN film.

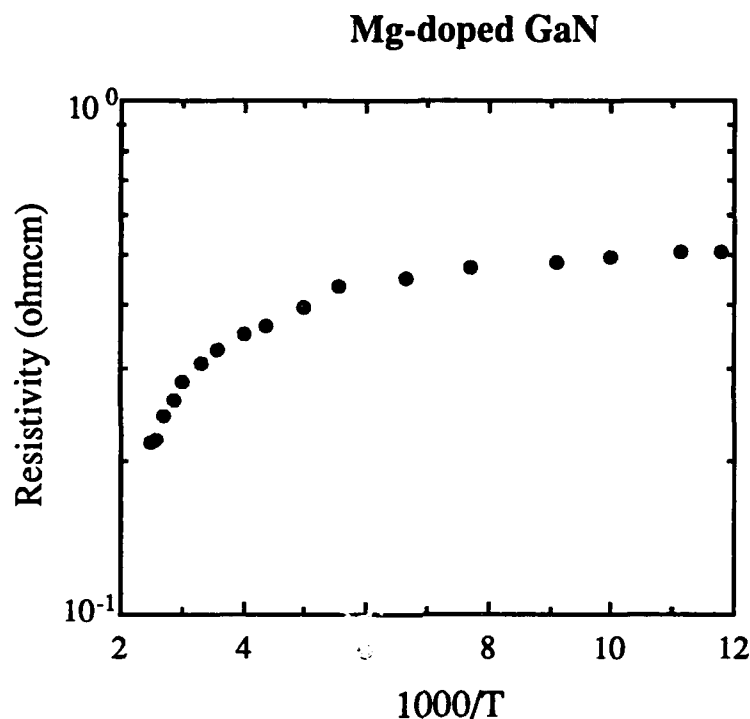


Figure 6. Temperature dependence of resistivity for a Mg-doped p-type GaN film.

D. Discussion

Undoped GaN films, made by different groups or by different deposition techniques, have been almost universally reported to be conductive and to exhibit n-type character. By contrast, as-deposited, Mg-doped GaN films resulted only in being compensated and were very resistive. No as-deposited p-type GaN films have been reported, even though a Japanese research group has reported that p-type conductive character as observed in Mg-doped GaN films which were treated by a post-deposition low-energy electron-beam irradiation [2]. Thus, the question is-raised as to why p-type GaN films can not be deposited directly. Moreover, what prohibits the activation of acceptor-like dopant. Finally, is the LEEBI treatment the only way to produce p-type GaN films and, if so, why? Answers to these questions are far from clear at this time.

Recently S. Nakamura et al. surmised that the acceptor-(e.g. Mg)H neutral complexes formed in as-deposited Mg-doped GaN films and were responsible for the unsuccessful p-type doping. In addition, these complexes were decomposed by a low-energy electron-beam irradiation. This resulted in the activation of the acceptor dopant and the achievement of p-type doping [8]. However, as yet they have provided no chemical evidence for the existence of hydrogen in their GaN films. We believe that the deactivation of the acceptor

dopant in the GaN films may also be related to the existence of a large density of defects, which could trap the acceptor-like dopants. Some of the dopant atoms may be weakly bonded to these defects. The LEEBI treatment, breaks these weak bonds and results in the activation of the acceptor dopant.

Our research group has also shown before [7] that, even under the best deposition conditions, undoped GaN films were still conductive and n-type while Mg-doped GaN films were very resistive acted and like an intrinsic film. Some changes were also observed after our LEEBI treatment, but not as dramatic as the Japanese group have reported. In contrast to these early research results, our recent work has shown that by eliminating the amorphous interfacial layer between the substrates and the deposited films, the crystalline quality of the deposited GaN film can be greatly improved. In this way, deposited undoped GaN films become intrinsic, while Mg-doped GaN films become p-type. This is further evidence that unsuccessful p-type doping for the past is mainly due to the existence of electrically activated microstructural defects in the deposited films.

It also should be pointed out that although the as-deposited p-type GaN films can be produced, the hole mobilities are quite low. Thus, are these the intrinsic properties of GaN films or can the film quality be further improved. It is well known that the lack of the lattice matched substrate materials for GaN make heteroepitaxy quite difficult. A large amount of lattice mismatch still exists even when AlN is used as the buffer layer. We believe that microstructural defects related to the lattice mismatch can be further reduced if we can find the "right" substrates, such as using a graded $\text{Al}_x\text{Ga}_{1-x}\text{N}$ solid solution as a buffer layer.

E. Conclusion

We have shown that in the use of our modified gas source MBE system, a thin layer of amorphous material was often formed by exposing the substrates to the nitrogen plasma prior to deposition. This could be prevented by exposing the substrate to Al prior to starting the nitrogen plasma. As a result, the deposited undoped GaN films showed intrinsic electrical character and were very resistive. Furthermore, by in-situ incorporation of Mg into the films, as-deposited p-type GaN films have been produced for the first time. The electrical properties of p-type GaN films were resistivity = $0.5 \Omega\text{-cm}$, Hall mobility = $10 \text{ cm}^2/\text{V}\cdot\text{s}$ and of carrier concentration $1 \times 10^{18} \text{ cm}^{-3}$ respectively.

F. Future Research Plans

As noted in the discussion part in this report, a graded $\text{Al}_x\text{Ga}_{1-x}\text{N}$ solid solution may also be chosen as the buffer layer for the homoepitaxy of GaN. Therefore, some of our future effort will involve the growth of good quality graded $\text{Al}_x\text{Ga}_{1-x}\text{N}$ solid solution buffer layers.

The purpose of this study will be to improve the hole mobility of the deposited GaN. Silicon will also be investigated as a donor dopant, and growth of n-type GaN films will be studied.

G. References

1. R. F. Davis, "Current Status of the Research on III-V Mononitrides Thin Films for Electronic and Optoelectronic Applications," in *The Physics and Chemistry of Carbides, Nitrides and Borides*, R. Freer, ed. Kluwer Academic Publishers, Dordrecht, The Netherlands, 1990, pp. 653-669.
2. H. Amano, M. Kito, K. Hiramatsu and I. Akasaki, *Jap. J. Appl. Phys.* **28**, 12112 (1989).
3. Z. Sitar, M. J. Paisley, D. K. Smith and R.F. Davis, *Rev. Sci. Instrum.* **61**, 2407 (1990).
4. Z. Sitar, L. L. Smith and R. F. Davis, "Morphology and Interface Chemistry of the Initial Growth of GaN and AlN on a-SiC and Sapphire," *MRS Symp. Proc.* (1991), to be published.
5. J. A Taylor and J. W. Rabalais, *J. Chem. Phys.* **75**, 1375 (1981).
6. S. Yoshida, S. Misawa and S. Gonda, *Appl. Phys. Lett.* **42**, 427 (1983).
7. R. F. Davis et. al., "The Effect of Electron Beam Irradiation on Mg Doped GaN Thin Films" in *Final Technique Report N00014-86-k-0686 P5*, 35 (1992).
8. S. Nakamura, N. Iwas, M. Senoh and T. Mukai, *Jpn. J. Appl. Phys.* **31**, 107 (1992).

III. Photo-assisted Growth of Gallium Nitride by Gas Source Molecular Beam Epitaxy

A. Introduction

Development and commercialization of light emitting diodes and semiconductor lasers has generated renewed interest in the more uncommon wide-bandgap III-V nitride semiconductors such as GaN. Since it has a band gap of ≈ 3.5 eV (near UV region) at room temperature and makes a continuous range of solid solutions with AlN (6.28 eV) and InN (1.95 eV), it is a promising material for devices for the emission of UV as well as visible radiation. It has long been thought that the high levels ($>10^{18}$ cm⁻³) of *n*-type conductivity and low resistivity ($<10^{-2}$ Ω -cm) were largely due to nitrogen vacancies produced during growth. This situation was exacerbated by the traditionally high temperatures used for CVD growth.[1, 2] More recent studies have used much lower growth temperatures that often gave much improved electrical properties.[3]

Use of photochemical processes for growth of thin films is a relatively recent development,[4] and as applied in MBE deposition, was characterized four years ago as being in its infancy.[5] Thus it is not surprising that extensive searches of the thin film semiconductor growth literature have shown only limited application of the potential photochemical effects that can be exploited. Current literature regarding the photo-enhanced growth of thin films can be classed into basic categories as: thermal effects (both equilibrium[6] and non-equilibrium,[7]) enhanced atom mobility,[8-10] photolytic and enhanced pyrolytic decomposition effects,[4] dopant activation,[11-13] and other photochemical effects.[14, 15] In many cases these effects are thought to occur in combination.[16, 17]

B. Experimental Procedures

1. Deposition System

The growth system was a commercial Perkin-Elmer 430 MBE system designed for 3" GaAs wafer handling but modified especially for the growth of nitrides. A resistively heated standard 20 cc effusion cell containing a BN crucible charged with 50 g of 99.999 999% pure gallium* was used for the evaporation of this component. An ECR microwave glow-discharge plasma source, designed and commissioned at NCSU,[18] was used to dissociate/activate the molecular nitrogen. This source was attached in place of a more traditional effusion (or cracker) cell for the group V element. The nitrogen gas was obtained from a compressed gas bottle of UHP-grade gas, passed through a resin bed purifier,† and subsequently regulated to the source by a variable leak valve.

*Rhône-Poulanc Specialty Chemical, Inc., South Brunswick, NJ 08852

†Nanochem L-50, Semigas Systems, San Jose, CA.

The most recent modification was the addition of a 500 W mercury arc lamp^{††} that was installed in front of a sapphire view port in the center of the source flange and oriented normal to the substrate. Figure 1(a) shows the spectral response of this particular lamp, while Figure 1(b) shows the transmission characteristics of the sapphire window.

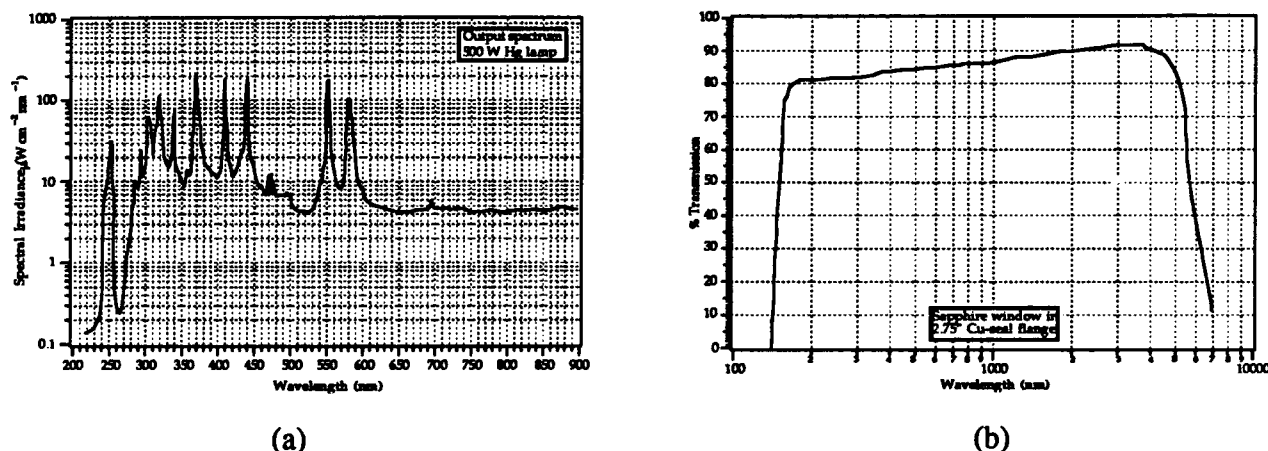


Figure 1. Optical spectra from components of the optical illumination system: (a) Hg-lamp output vs. wavelength (used with permission, Oriel Corporation), and (b) transmission vs. wavelength of sapphire window, (used with permission, Perkin-Elmer Corporation).

Calculations were made to estimate the illumination intensity at the growth surface. This involved integration of the area under the curve in FIG. 1(a), accounting for the lamp mirrors, condensing optics, sapphire window, and lamp-to-substrate distance (50 cm). This resulted in an estimated illumination intensity using the entire spectrum of Figure 1(a) of ~ 0.4 W/cm². This value does not account for spherical and chromatic aberration losses in the optical path nor minor gains from the metal tube in the source flange cryoshroud that extends from just behind the sapphire window toward the substrate for a distance of 15 cm.

2. Substrate Preparation and Growth

Growth studies were conducted on (100)-oriented β -SiC (zincblende structure) films that were epitaxially grown on (100) Si substrates (12 mm dia. \times 0.5 mm) by CVD of Si and C from pyrolysis of highest purity SiH₄ and C₂H₄ entrained in H₂ in an rf-heated cold-wall barrel-type reactor. These substrates were polished with 0.1 μ m diamond paste and subsequently oxidized at 1200°C in flowing dry oxygen for 1.5 h to consume the 50 nm of surface which contained subsurface polishing damage within a layer of silicon oxide \approx 100 nm thick. A more detailed description of the sample preparation has been presented in an earlier paper.[19] The oxide was removed in a 49% HF etch and loaded into the system.

^{††}Model 6285 lamp in Model 66042 housing, Oriel Corporation, Stratford, CT 06497

After outgassing, the samples were introduced into the growth chamber and examined using the *in situ* reflection high energy electron diffraction (RHEED) system using a 10 kV beam. The resulting RHEED pattern on the β -SiC substrate showed Kikuchi lines indicative of the good crystalline quality of the substrate. The range of conditions used during growth is presented in Table I.

TABLE I. Conditions used in GaN growth

Nitrogen pressure	2×10^{-4} Torr
Microwave power.....	50 W
Gallium temperature.....	975 or 990°C
Substrate temperature.....	600°C
Growth time.....	180 min.

After the growth was complete, the sample was again evaluated with RHEED to determine crystal structure and to get an initial estimate of film quality.

3. Thin Film Analysis

Chemistry and Morphology. The XPS spectra in Figure 2 show no noticeable differences between films deposited with and without the lamp illumination. Higher resolution scans around the O_{1s} and C_{1s} peaks (not shown) revealed undetectable levels of contamination in both cases. Thus further XPS analysis was not performed.

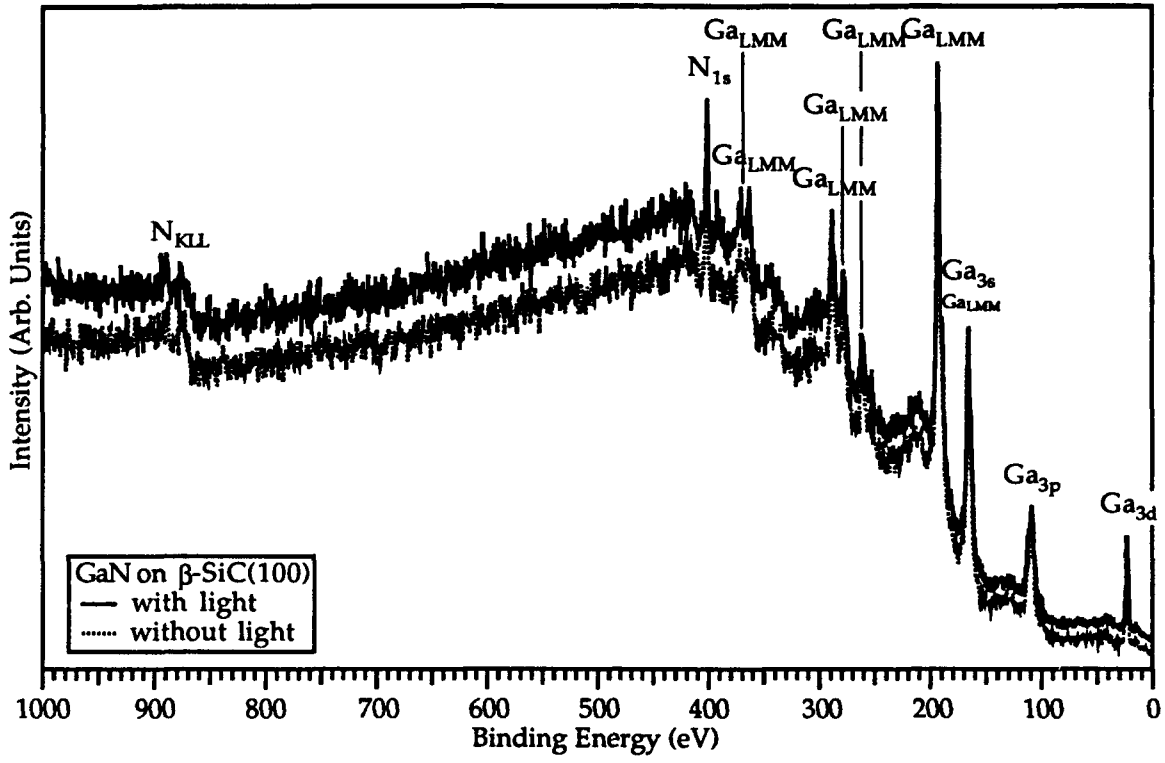


Figure 2. XPS spectra of GaN on β -SiC(100) deposited with and without illumination during deposition from a 500-W Hg-arc lamp.

Field emission SEM* examinations of samples grown using the two different cell temperatures are shown in the following figures. Films deposited at Ga cell temperature of 975°C and 990°C and without substrate illumination are shown in Figure 3, and those with illumination are shown in Figure 4. The film deposited at the Ga cell temperature of 990°C appears free of gross features in Figure (a), but the higher resolution image in Figure (b) shows a random angular texture indicative of a polycrystalline film with an apparent grain size of $\approx 0.1 \mu\text{m}$. The micrograph of the film grown using a Ga temperature of 975°C is presented in Figure (c) shows a completely different morphology with long narrow pores scattered across the surface. Figure (d) also shows what appears to be two rectangular domains oriented at 90° to each other with additional, much smaller, equiaxed regions interspersed.

* Hitachi S-4000, Hitachi Corp., Tokyo, Japan.

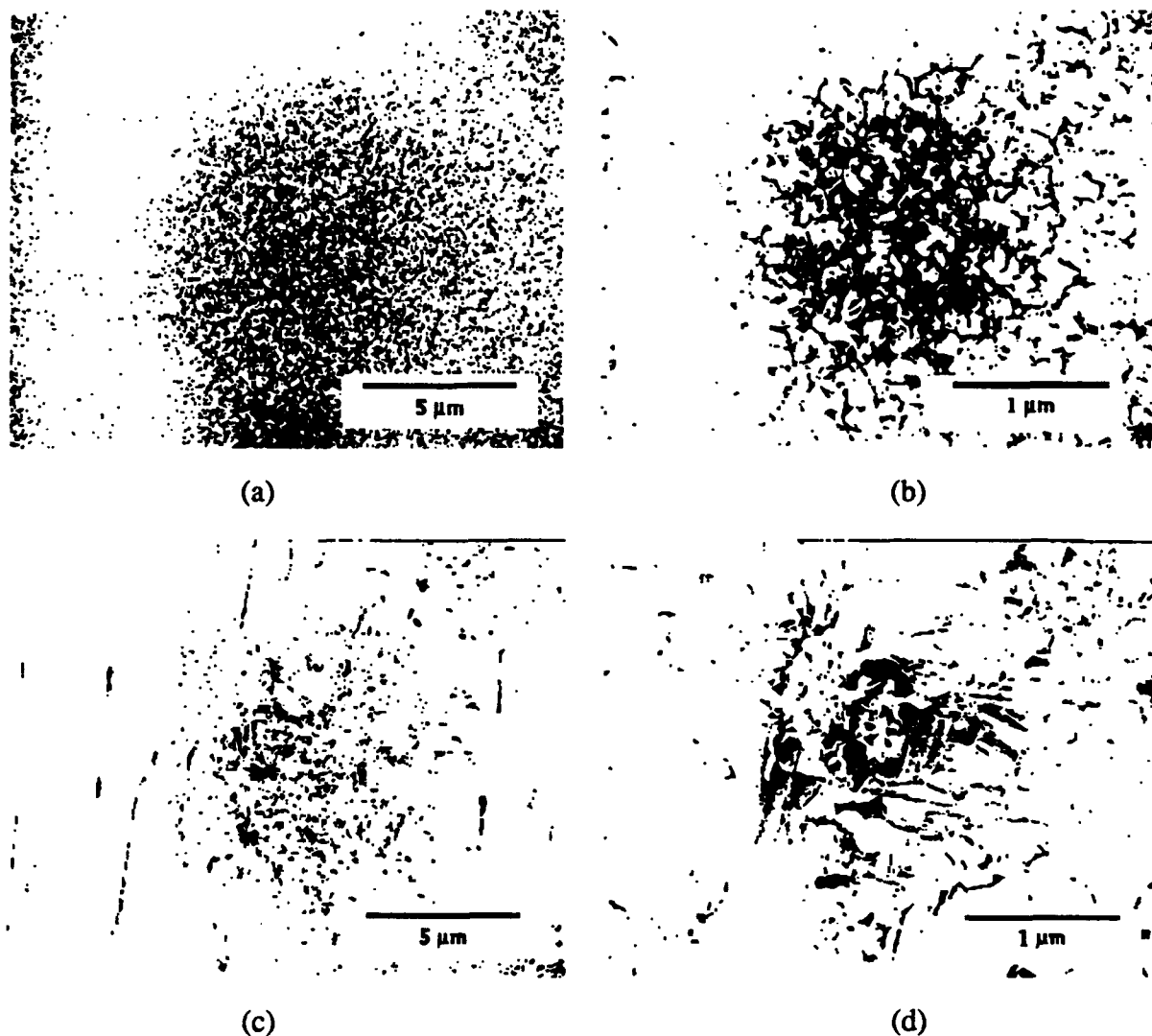


Fig. 3. SEM photographs of GaN surface morphology deposited without illumination: (a&b) 990°C Ga cell temperature; (c&d) 975°C Ga cell temperature.

The surface morphology of the films might be expected to be quite different for films deposited with illumination from the lamp, if surface mobilities are changed. This effect is clearly demonstrated in Figure (a-d). The films are basically free from gross features which cannot be related to defects in the substrate surface, but the fine structure of the morphology is unrelated to the substrate surface. At a Ga temperature of 990°C the film shown in FIG. 4(a&b) is clearly polycrystalline, but the grains appear to have a preferred orientation or texture. This is different from the random texture observed in the film shown in Figure (a&b). The 975°C Ga temperature film shown in Figure (c&d) shows a radically different morphology than any of the earlier films. The surface is much smoother and more uniform with only small islands extending a small distance above the surface of the film.

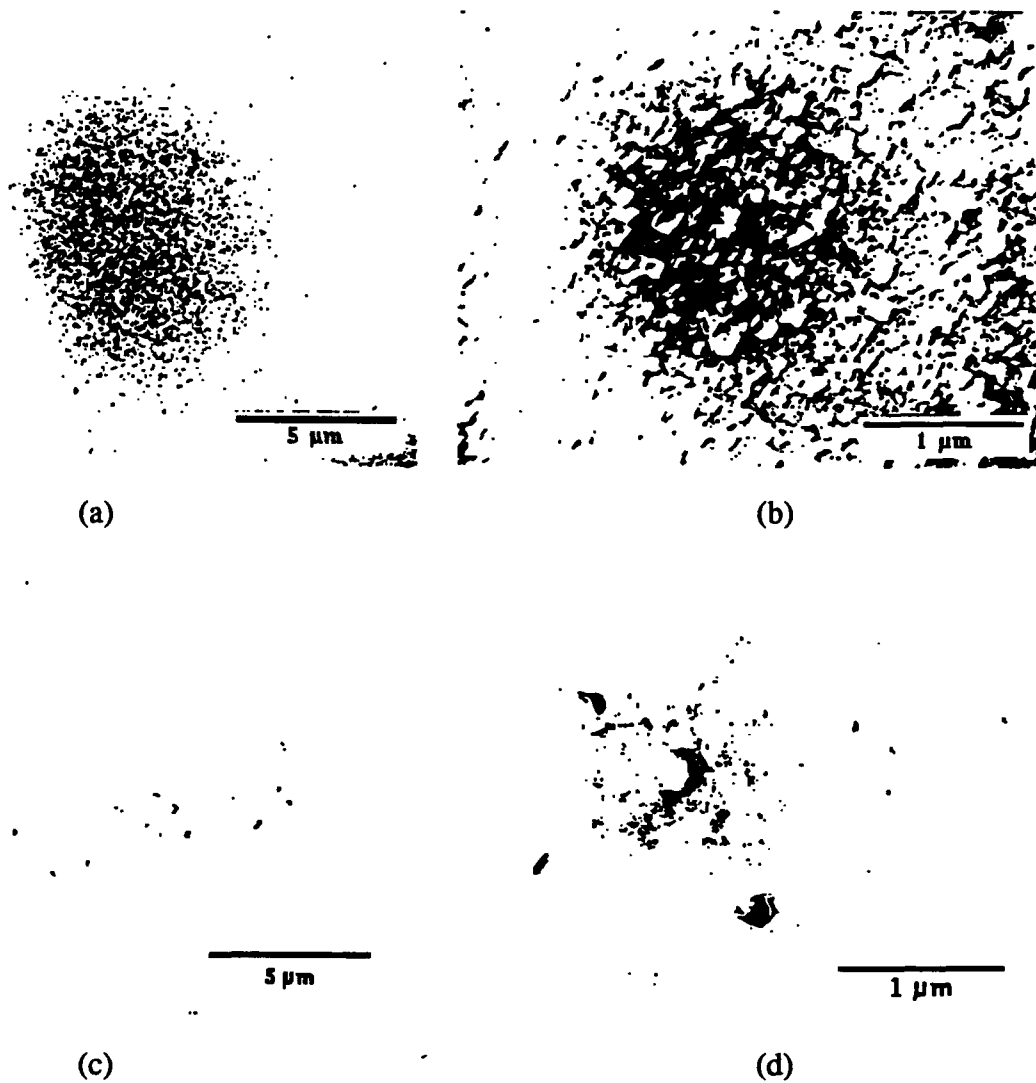


Figure 4. SEM photographs of GaN surface morphology deposited with lamp illumination: (a&b) 990°C Ga cell temperature; (c&d) 975°C Ga cell temperature.

Figure 4(a–d) show a different granular texture, due to the effects of the photon irradiation. The features appear much smoother than the previous example, and have, on average, a different shape than films deposited without illumination in Figure (a–d).

Subsequently the films were cleaved along one of the {011}-type planes and mounted with the freshly cleaved surface so that it could be viewed in an SEM.[†] They were examined in the backscattered imaging mode to determine the thickness of the films deposited under the two Ga cell temperatures. Since the average atomic numbers (\bar{Z}) for GaN and SiC are 17 and 10, respectively, the backscattered image of the GaN layer is brighter than the SiC

[†]Model JSM-6400F, JEOL, Inc., Tokyo, Japan.

substrate. The results (which include measurements from cross-section TEM discussed later) are shown in Table II.

Table II. Thicknesses of GaN layers deposited under listed conditions measured by backscattered electron imaging (BEI) and cross-sectional TEM.

Conditions	BEI	XTEM
Ga@990°C w/o light	550 nm	550 nm
Ga@990°C w/ light	500 nm*	450-500 nm*
Ga@975°C w/o light	400 nm	420 nm
Ga@975°C w/ light	360 nm	350 nm

*Increased surface roughness made this measurement difficult.

This table shows that light illumination during growth decreased the resulting film thickness by $\approx 10\%$ at both Ga cell temperatures, and that changing the Ga cell temperature by 15°C decreased the resulting film thickness by $\approx 25\%$, regardless of the use of illumination. The decrease in film thickness due to the reduction in Ga cell temperatures corresponded to the expected change in Ga vapor pressure according to interpolations of published vapor pressure data.[20] The effect of the illumination on the final film thickness is a much more confusing situation since, as mentioned in the introduction, there are a number of potential competing effects.

However, some effects can be safely eliminated. Pure thermal effects can safely be discarded since the illumination intensity is too low ($<0.5 \text{ W/cm}^2$) for bulk heating of the substrate. Pyrolytic effects can also be discarded as important in this case, since the wavelengths emitted by the lamp are not sufficiently short to produce excited nitrogen or gallium atoms.[21] Dissociation of Ga_2 vapor is possible[22] but gallium was observed to evaporate as an atomic species using an *in situ* quadrupole mass spectrometer.§

A reduced film thickness as a result of enhanced desorption caused by laser illumination (300 mW/cm^2 at 441.6 nm) was observed in the $\text{ZnS}_x\text{Se}_{1-x}$ system by Matsumura, Fukada, and Saraie.[10] And this phenomenon is believed to be the explanation for the reduction in thickness in the films of the present study. However the Japanese investigators observed much more dramatic thickness changes of 50–60% (at somewhat lower intensities). Their modeling showed a greatly increased desorption rate for the physisorbed species and only a slight increased desorption for the chemisorbed species. Since the resultant surface morphology for GaN indicates that adatom mobility is increased and thereby implies that desorption becomes more favorable, then some other factor retards the desorption of the Ga-N surface species relative to that in the $\text{ZnS}_x\text{Se}_{1-x}$ system. Since the vapor pressure of

§ Model 100, UTI Corp., Milpitas, CA.

Ga is much lower than that of either Zn, S, or Se, it seems likely that its energy of physisorption would be higher, leading to a lower probability of desorption.

Structural Analysis. The polycrystalline nature of these films was confirmed by RHEED performed after growth, which showed a clear sharp ring pattern except for the film grown at the lower Ga temperature and with illumination. This film showed a pattern indicating two superimposed single crystal patterns.

X-ray diffraction patterns were taken of each film and are shown in Figure 5. Note that all curves have been normalized to the intensity of the Si (400) peak. The intensity of the wurtzitic GaN (w-GaN) reflections varied dramatically and in an unusual manner with respect to deposition conditions.

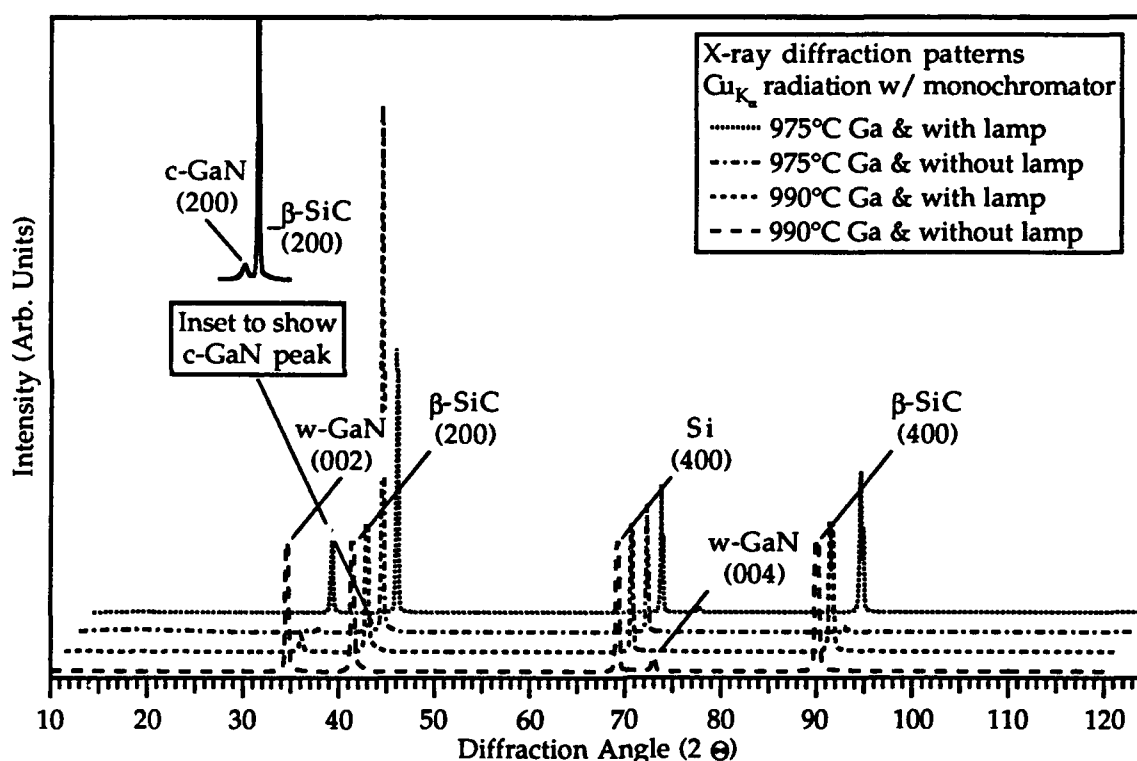


Figure 5. X-ray diffraction patterns of GaN films on epitaxial β -SiC on Si (100) using $\text{CuK}\alpha$ radiation. Patterns have been normalized to the intensity of the Si (400) reflection.

Film growth at 990°C Ga temperature and without illumination showed a strong w-GaN (0002) peak and a weaker w-GaN (0004) peak. This would imply a strong texture of w-GaN (0002) || β -SiC (100) in the deposited film. No other texture information was derived from this measurement since it was limited to in-plane lattice spacings, though RHEED and SEM revealed that it was polycrystalline.

Deposition at the 990°C Ga temperature but with illumination showed a dramatically weaker w-GaN (0002) peak and the w-GaN (0004) peak was no longer present.

Deposition at the 990°C Ga temperature but with illumination showed a dramatically weaker w-GaN (0002) peak and the w-GaN (0004) peak was no longer present. Interestingly, no other w-GaN peaks appeared, indicating a strong texturing about a plane (or planes) with low scattering power that do not produce detectable reflections due to the thinness of the deposited layer. It could be argued that the lack of peaks is due to the thinness of the layer and a random orientation of the grains producing reflections too weak for detection. This is unlikely, as there are five peaks with relative intensity of $\geq 80\%$ (two are 100%) in the w-GaN pattern,[†] making observation of these other peaks fairly easy. In addition, the SEM photographs in FIG. 4(a&b) indicated a strong texturing of the film.

Film growth at the 975°C Ga temperature and without illumination also showed a very weak w-GaN (0002) peak but no w-GaN (0004) peak, and an additional small β (cubic)-GaN (200) peak. There is no JCPDS standard pattern for c-GaN, but zincblende structures in general have a much stronger (111) peak than (200) peak, indicating a strongly textured orientation of both polymorphs of the GaN film to the substrate. This texturing was also evident in the SEM photographs of Figure 3(c&d).

Deposition at the 975°C Ga temperature and with illumination showed a strong w-GaN (0002) peak, a weak w-GaN (0004) peak, and no others that indicated a strong texturing of the film to the substrate. This was borne out by the SEM photographs in Figure 4(c&d), showing the hexagonal islands scattered across the surface.

Transmission electron microscopy* (TEM) was used to further assess the microstructure of the GaN epitaxial films. Cross-section TEM specimens were prepared using standard techniques.[23] Preliminary evidence for a new polytype of w-GaN will be presented. This polytype (as observed) has lattice parameters of $a=0.318$ nm and $c=1.033$ nm, or the same parameters as normal wurtzitic (2H) GaN, but with a c -axis $2\times$ larger than normal. This is due to a modified stacking sequence. Normal wurtzite has a stacking sequence of $abab$, while 4H material has a stacking sequence of $abcb$ (or the equivalent $abac$). Thus 4H-GaN can be interpreted as either wurtzitic GaN with regular stacking faults or atom-layer twinned cubic GaN (the ultimate micro-twin). The evidence for this new polytype is in the form of an additional diffraction spot observed at one-half the radial distance for the normal w-GaN (0002) reflection. Half-order diffraction spots are sometimes observed in hexagonal materials as a result of double diffraction.[24] However, tilting experiments have shown that though double diffraction was still possible, it was unlikely to be the cause.

Figure 6 shows the SAD pattern from a single grain of GaN from the film deposited at a 990°C Ga cell temperature without illumination superimposed upon the β -SiC substrate pattern. When compared to the modeled pattern on the right, this pattern shows that the

[†] Card #2-1078, JCPDS-ICDD, (1989).

* H-800 STEM, Hitachi Corp., Tokyo, Japan.

orientation is w-GaN (0001)|| β -SiC(100) (all grains) and (10 $\bar{1}$ 0)|| $(01\bar{1})$ (this grain). This same texture was also observed in the x-ray diffraction data in Figure 5. Note that the w-GaN (0002) spots are at one-half their normal distance, indicating rather than a true wurtzite (2H) phase a related 4H-GaN phase was formed. TEM observations in other areas confirm that the film is polycrystalline but the film maintains the basal orientation mentioned above and nearly random otherwise. The w-GaN (0001) is the close-packed plane in this structure and so it would be the lowest surface energy plane. Thus it appears that the surface energy considerations are dominant over strain effects in this growth regime.

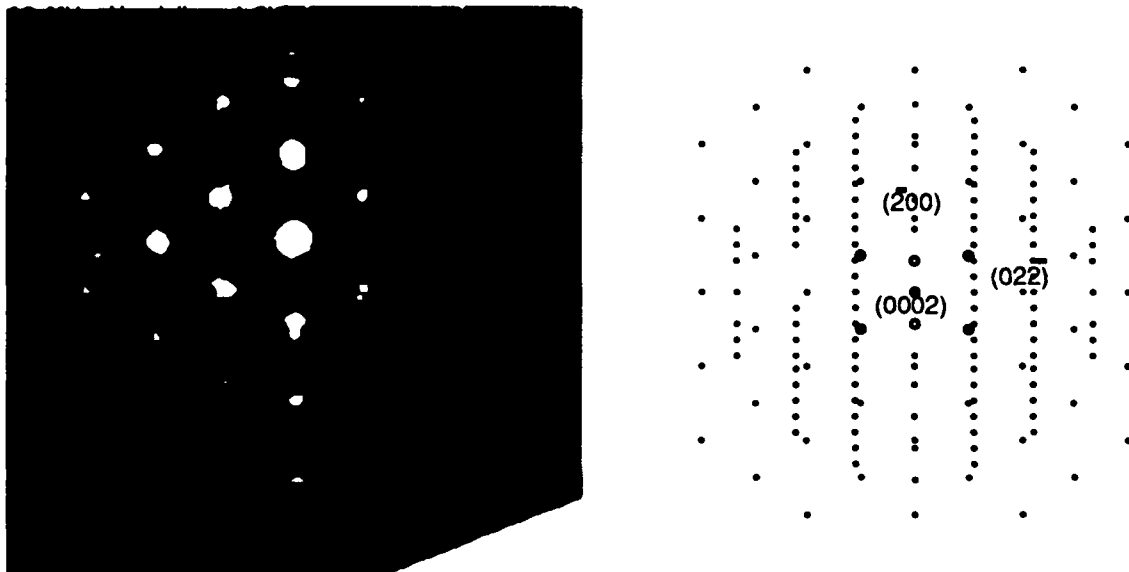


Fig. 6. Cross-section SAD pattern from one polycrystalline grain of GaN on β -SiC (100) at higher Ga cell temperature without illumination during growth. Left: Real SAD pattern. Right: Model showing orientation ($z=[011]$).

Figure 7 shows the cross-section SAD pattern of a polycrystalline region from the film at the 975°C Ga temperature without illumination during growth. The pattern is shown with the substrate and reveals two unique orientations of w-GaN to the substrate. Dim spots near the transmitted spot confirmed the continued presence of 4H-GaN from the (0002) reflection. The orientations found in the film were c-GaN: (200)|| β -SiC (200) and (220)|| (220) (not shown); one set of w-GaN: (0001)|| β -SiC ($1\bar{1}1$) and $(01\bar{1}3)||100$; and the other set of w-GaN: (0001)|| β -SiC ($11\bar{1}$) and $(01\bar{1}3)||(\bar{1}2\bar{2})$. These w-GaN orientations would not provide planes parallel to the surface with any scattering power and thus explains the lack of peaks from the x-ray data in Figure 5. Since the close-packed planes in the w-GaN are aligned to the close-packed planes in the substrate, it seems that strain effects are dominant in this growth regime, where the film begins to follow the template of the substrate more closely, as opposed to the surface energy effects discussed earlier.

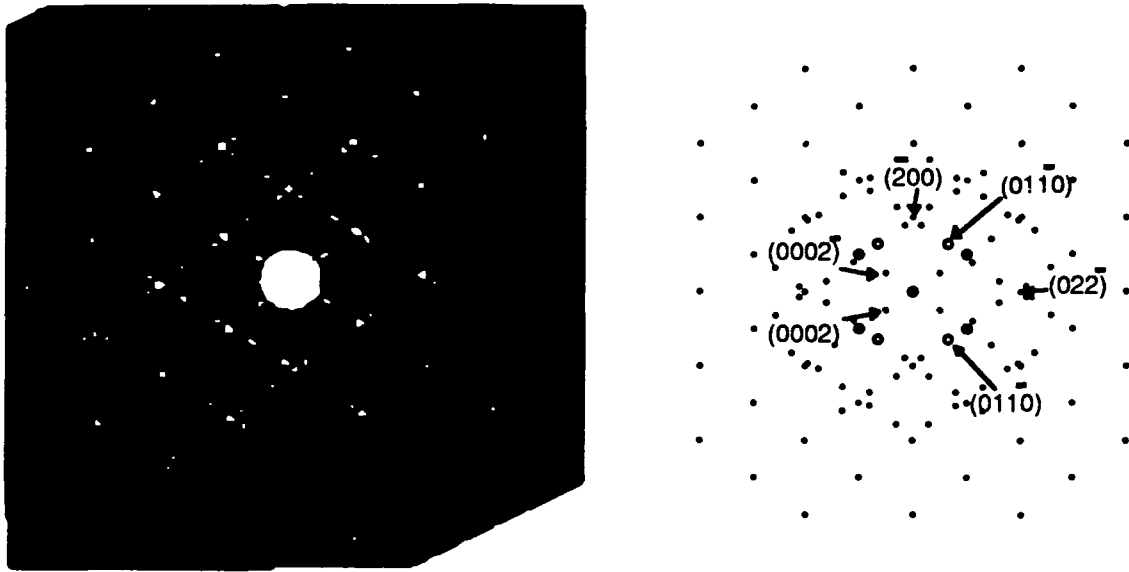


FIG. 7. Cross-section SAD pattern from polycrystalline patterns of 4H-GaN on β -SiC (100) at the lower Ga temperature without illumination during growth. Left: Real pattern. Right: Model showing orientation ($z=[011]$).

Addition of illumination of the growth surface during deposition changed the observed orientation effects dramatically. Figure 8 is a cross-section SAD pattern from the film grown at the 990°C Ga temperature and with illumination. Very dim spots near the center confirm the continued presence of 4H-GaN from the (0002) reflection. The three spotted rings corresponded to the $(1\bar{0}0)$, $(1\bar{0}1)$, and $(2\bar{0}2)$ planes of w-GaN. This pattern appears to have elements of orientation as seen in Figure 7 as well as some texture observed earlier in Figure 6. Thus the lack of peaks in the x-ray data (see Figure 5) is due to multiple orientations of peaks with low scattering power. There is an additional orientation indicated by the presence of the $(1\bar{0}1)$ ring which is not easily explained. Interpretation of the significance of this texture is difficult, since the $(1\bar{0}1)$ was not observed in any of the other growth conditions. It would appear that this particular growth was in a transition region where multiple mechanisms were active.

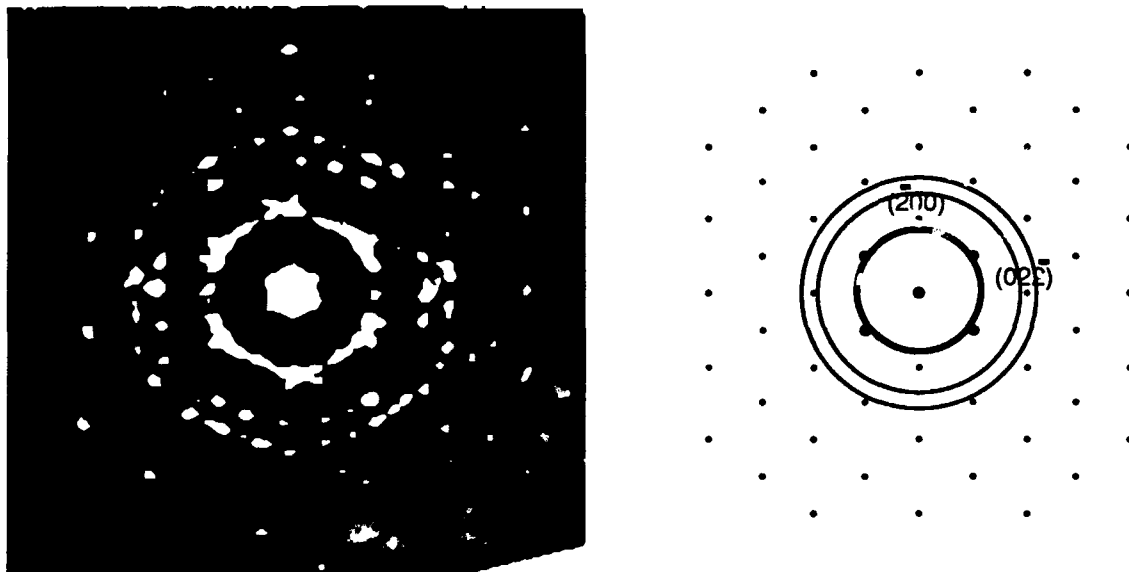


FIG. 8. Cross-section SAD pattern from a polycrystalline region of w-GaN deposited at the higher Ga temperature and with illumination, superimposed upon the β -SiC substrate pattern ($z=[011]$). Left: Real pattern. Right: Model showing orientation ($z=[011]$).

Figure 9 is a cross-section SAD pattern from the film grown at the 975°C Ga temperature and with illumination. The orientation relationship was found to be w-GaN (0001) || β -SiC (100) and $(10\bar{1}0)$ || $(01\bar{1})$. Since this orientation places the w-GaN (0001) planes parallel to the surface, it would provide a strong w-GaN (0002) reflection as observed in Figure 5. This relationship is somewhat unexpected as the film shown in Figure 6 had assumed a similar orientation without illumination, but with addition of the photon irradiation, it changed to a mixed one as illustrated in Figure 8. Furthermore, since the β -SiC(100) surface has four-fold symmetry and the 4H-GaN(0001) surface has six-fold symmetry the 4H-GaN must follow a two-dimensional coincidence boundary rather than a more regular alignment of lattice sites on the surface. It should be noted that this film is very near to being a single crystal, with only mild broadening of the higher order diffraction spots.

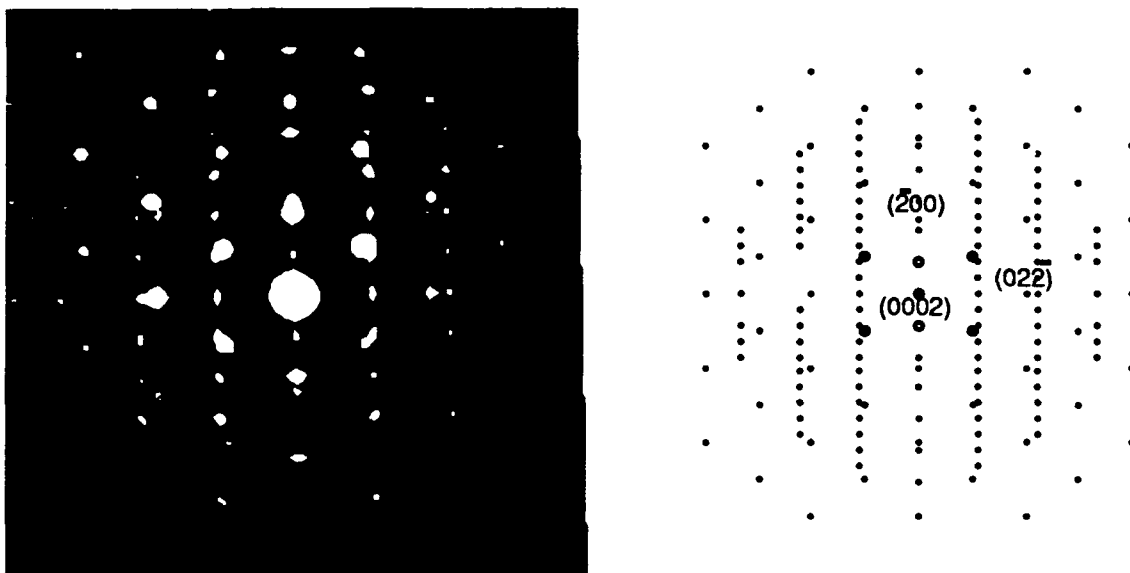


FIG. 9. Cross-section SAD pattern from a near single crystal 4H-GaN on β -SiC (100) at a 975°C Ga temperature with illumination during growth. Left: Real pattern. Right: Model showing orientation ($z=[011]$).

C. Summary

Thin films of GaN were grown on β -SiC (100) substrates at different Ga cell temperatures in a modified MBE system using nitrogen flowing through a compact microwave ECR source. Films illuminated during growth by a 500 W Hg arc lamp were changed in the resulting structural arrangement and surface morphology observed in the GaN films. The illumination reduced the growth rate of the films by $\approx 10\%$ and also changed the observed texturing orientation of the deposited film to the substrate. It appeared that in this deposition regime there is strong competition between surface energy and strain energy effects on the resulting film texture. Illumination of the growth surface from the broad band emission of the 500 W Hg arc lamp increased the quality of the w-GaN toward single crystal with a resulting film orientation on β -SiC of w-GaN (0001) \parallel β -SiC (100) and (10 $\bar{1}$ 0) \parallel (01 $\bar{1}$).

D. Acknowledgments

The authors wish to express their appreciation to Mr. Max Yoder (ONR) for his many helpful discussions and worthwhile suggestions. Thanks are also extended to Dr. Zlatko Sitar for his insight and suggestions. This work was sponsored by the SDIO/IST and managed by ONR under contract No. N00014-86-K-0686.

E. References

1. H. P. Maruska and J. J. Tietjen, *Appl. Phys. Lett.* **15**(10), 327 (1969).
2. J. I. Pankove and P. E. Norris, *RCA Rev.* **33**, 377 (1972).
3. S. Strite, *et al.*, *J. Vac. Sci. Technol. B* **9**(4), 1924 (1991).
4. R. Solanki, C. A. Moore, and G. J. Collins, *Sol. State Technol.* **28**(6), 220 (1985).

5. B. A. Joyce, *J. Phys. Chem. Solids* **49**(3), 237 (1988).
6. A. I. Kingon, O. Auciello, M. S. Ameen, S. H. Rou, and A. R. Krauss, *Appl. Phys. Lett.* **55**(3), 301 (1989).
7. A. Lietoila, R. B. Gold, J. F. Gibbons, and L. A. Christe, in *CW Beam Processing of Silicon and Other Semiconductors* J. F. Gibbons, Eds. (Academic Press, New York, 1984), pp. 71.
8. Z. Yu and G. J. Collins, *Phys. Scripta* **41**(1), 25 (1990).
9. M. Kitagawa, Y. Tomomura, K. Nakanishi, A. Suzuki, and S. Nakajima, *J. Cryst. Growth* **101**, 52 (1990).
10. N. Matsumura, T. Fukada, and J. Saraie, *J. Cryst. Growth* **101**(1-4), 61 (1990).
11. N. C. Giles, *et al.*, *J. Cryst. Growth* **86**(1-4), 348 (1988).
12. N. C. Giles, K. A. Bowers, R. L. Harper Jr., S. Hwang, and J. F. Schetzina, *J. Cryst. Growth* **101**(1-4), 67 (1990).
13. S. Fujita, A. Tanabe, T. Kinoshita, and S. Fujita, *J. Cryst. Growth* **101**(1-4), 48 (1990).
14. T. Wolkenstein, *Adv. Catal. Rel. Subj.* **23**, 157 (1973).
15. S. R. Morrison, *J. Catal.* **20**, 110 (1971).
16. T. Y. Sheng, Z. Q. Yu, and G. J. Collins, *Appl. Phys. Lett.* **52**(7), 576 (1988).
17. T. Yamazaki, S. Watanabe, and T. Ito, *J. Electrochem. Soc.* **137**(1), 313 (1990).
18. Z. Sitar, M. J. Paisley, D. K. Smith, and R. F. Davis, *Rev. Sci. Instrum.* **61**(9), 2407 (1990).
19. M. J. Paisley, Z. Sitar, C. H. Carter Jr., and R. F. Davis, in *SPIE's OE/LASE—Innovative Science and Technology Symposium*. C. A. Kukkonen, Eds. (SPIE-The International Society for Optical Engineering, Los Angeles, CA, 1988), pp. 8.
20. R. Glang, in *Handbook of Thin Film Technology*, L. I. Maissel, and R. Glang, Eds. (McGraw-Hill, New York, 1970), pp. 1.
21. H. Okabe, *Photochemistry of Small Molecules* (Wiley-Interscience, New York, 1978).
22. W. A. Young, M. Y. Mirza, and W. W. Duley, *Opt. Commun.* **34**(3), 353 (1980).
23. J. C. Bravman and R. Sinclair, *J. Electron Microsc. Techniq.* **1**, 53 (1984).
24. G. Thomas and M. J. Goringe, *Transmission Electron Microscopy of Materials* (Wiley-Interscience, New York, 1979), p. 88.

IV. Deposition of Cubic Boron Nitride

A. Introduction

Cubic boron nitride is a material with potential applications due to both its tribological and electronic properties. It is the hardest material other than diamond, and it is more stable than diamond at higher temperatures. It does not react with the ferrous metals, which makes it an ideal cutting tool material. For electronic applications, it is of interest because it is a good insulator with very high thermal conductivity; yet it also has the potential of being doped as both a p-type and n-type semiconductor. Boron nitride is similar to carbon in having three basic structures, an sp^2 bonded layered hexagonal structure (h-BN) corresponding to graphite, the sp^3 bonded cubic structure (c-BN) corresponding to diamond, and a rare sp^3 bonded hexagonal wurtzite structure (w-BN) which corresponds to Lonsdaleite. The layered hexagonal structure is typically referred to simply as hexagonal BN. There are also variations of these structures, the most important one for this study being turbostratic BN (t-BN), which, like hexagonal BN, consists of sp^2 bonded layers, but in which the layers are randomly oriented to each other [1].

Bulk cubic boron nitride was first synthesized in 1956 using high pressure-high temperature methods [1]. In recent years, reports have appeared of cubic boron nitride grown in thin film form, using both chemical vapor deposition (CVD) and physical vapor deposition (PVD) methods [2-6].

In this work we are attempting to grow cubic boron nitride that can be used for electronic applications. This leads to different priorities from those researchers studying cubic boron nitride for tribological applications. For electronics applications the primary concerns are phase purity, grain size, compositional purity, sharp interfaces, and electrical properties.

We have successfully grown cubic boron nitride using ion beam assisted deposition (IBAD). We have also attempted to develop an understanding of the c-BN growth process and the factors influencing it.

B. Experimental Procedure

1. Film Growth

A UHV ion beam assisted deposition (IBAD) system was used for film deposition. Samples were loaded through a load lock system. Base pressures in the chamber were typically $< 1 \times 10^{-9}$ Torr. Boron was deposited by evaporating boron metal using an electron beam evaporator. Simultaneously a Kaufman type ion gun was used to bombard the depositing boron with both nitrogen and argon ions. The films were deposited onto heated substrates. A schematic of the setup is shown in Figure 1. The deposition rate of the boron, the energy and flux of the ions, the ratio of the argon to nitrogen, and the substrate temperature were all measured, controlled, and varied. The boron was evaporated using a Thermionics HM2 electron gun with an electromagnetic beam sweep. The boron was in a graphite crucible liner which was in a water cooled 10 cc crucible. It was deposited at a rate of from 0.25 to 1.0 Å/s. The deposition rate was monitored using a quartz crystal monitor.

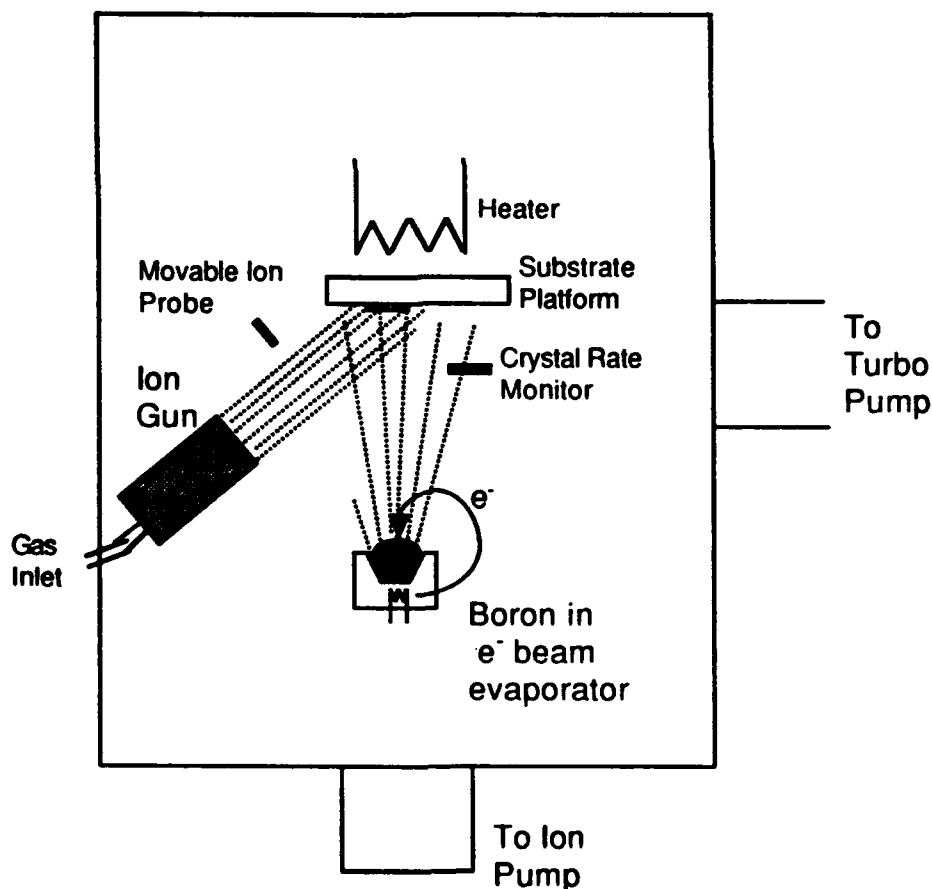


Figure 1. Schematic of deposition system.

The film was bombarded using an Ion Tech 3 cm Kaufman ion source. Bombardment was by either nitrogen and argon or nitrogen and krypton ions in varied ratios, all at 500 eV. The

flux of ions ranged from 0.05 to .30 mA/cm² and was measured using a negatively biased ion probe. The gas flow to the ion gun was 1.5 sccm for each of the two gases and was controlled using MKS mass flow controllers. Typical deposition pressures in the chamber were 1.0×10^{-4} Torr.

Substrates were heated from 300 to 700°C. The substrates used were 100 silicon wafers with high resistivity (25-45 Ω -cm) so as to be transparent for IR spectroscopy. Film thicknesses ranged from 100Å to 2000Å.

2. Film Characterization

FTIR. Fourier transform infrared spectroscopy (FTIR) has been found to be the best method for the purpose of determining whether a deposited film is cubic or hexagonal boron nitride. With FTIR analysis the cubic and hexagonal forms of boron nitride give distinct, independent peaks, due to the sp³ and sp² bonds, respectively. Hexagonal boron nitride has absorption peaks at 1367 cm⁻¹ and at 783 cm⁻¹ [1], while cubic boron nitride has a transverse optical mode absorption peak at 1075 cm⁻¹ [2].

Transmission Electron Microscopy. Structural characterization was studied by high resolution transmission electron microscopy. Cross-sectional samples of the BN thin films grown on Si(100) substrates were prepared using standard techniques. High resolution TEM was performed in a TOPCON EM-002B operated at 200 kV. Selected area diffraction (SAD) was used to characterize the structure of the film, however, data was needed from more limited areas than what was obtained with this technique. Therefore, after printing the images, they were digitized by scanning them into a Macintosh IIfx computer using an Apple OneScanner with *Ofoto v1.0* scanning software. The software package *Image v1.28b6* with the FHT extension was used to obtain diffraction information from the images in the form of a fast Hartlee transform, FHT (which is similar to a fast Fourier transform).

Electrical. Electrical measurements of the films consisted of I-V measurements performed using a mercury probe with a large and a small area contact

Rutherford Backscattering. The stoichiometry of the films was measured using Rutherford backscattering (RBS), in which helium nuclei are used to bombard the film. By measuring the energy and angle of the backscattered nuclei, information about the film composition can be determined. RBS is particularly useful in that it gives a depth profile of the film, not only information about the surface layer.

C. Results

1. Varying Bombardment Gases

The conditions which lead to cubic boron nitride occur, for a give substrate temperature, in a parameter window of momentum transferred into the film by the bombarding ions [3]. At 400°C this window is from 200-300 (eV × amu)^{1/2}. The lower boundary of this window is where films go from being hexagonal to being cubic. At the upper boundary of this window the bombardment is of an intensity that it leads to complete resputtering of the deposited material. Optimizing the deposition conditions for c-BN deposition means finding the boundaries of this window, and attempting to widen that window. The best parameter to vary in order to control the momentum value is the ratio of ions bombarding the film to boron atoms depositing. This is due to the momentum varying in direct proportion to changes in this ratio, while only varying as the square root of the ion energies or masses, the other major factors contributing to the value of the momentum. This ion to atom ratio can be controlled directly by varying either the boron deposition rate or the ion beam current.

Finding the boundaries of the parameter window was straightforward, trying to widen it is proving more difficult. One method attempted was replacing argon, the bombarding gas generally used in addition to nitrogen, with krypton. Calculations as well as earlier results using two ion guns had indicated that this could be a successful method [3]. Our work in this regard was unsuccessful in getting any better results than by using argon with nitrogen. It is suspected that the lack of positive results is due to using nitrogen and krypton simultaneously in the same ion gun. Because of the difference in ionization potentials between these two gases, the relative distributions of the ions coming out of the gun becomes very difficult to control. Specifically it is expected that almost all the ions will be krypton. This problem is avoided when using argon with nitrogen, since these two gases have very similar ionization potentials.

2. Effects of Film Thickness

In studying the effects of depositing c-BN at different thicknesses, it was found that for very thin films (~125Å) the relative amount of hexagonal phase in the films, as determined by FTIR, was high. As the thickness increased, the relative percentage of cubic phase increased (Figure 2). This suggested that films were initially depositing as a mixed cubic-hexagonal phase film, becoming mainly cubic at a later stage of deposition. Examination of the films using high resolution TEM (Figure 3) revealed that the films actually consisted of three layers, an initial layer of about 20Å amorphous BN at the silicon interface, followed by a layer of what appears to be hexagonal or turbostratic BN, followed by growth of apparently polycrystalline cubic material. FHT (Fast Hartlee Transform) was performed on the HRTEM match that of c-BN, while the middle layer matched that of turbostratic BN (t-BN) (Figure 4).

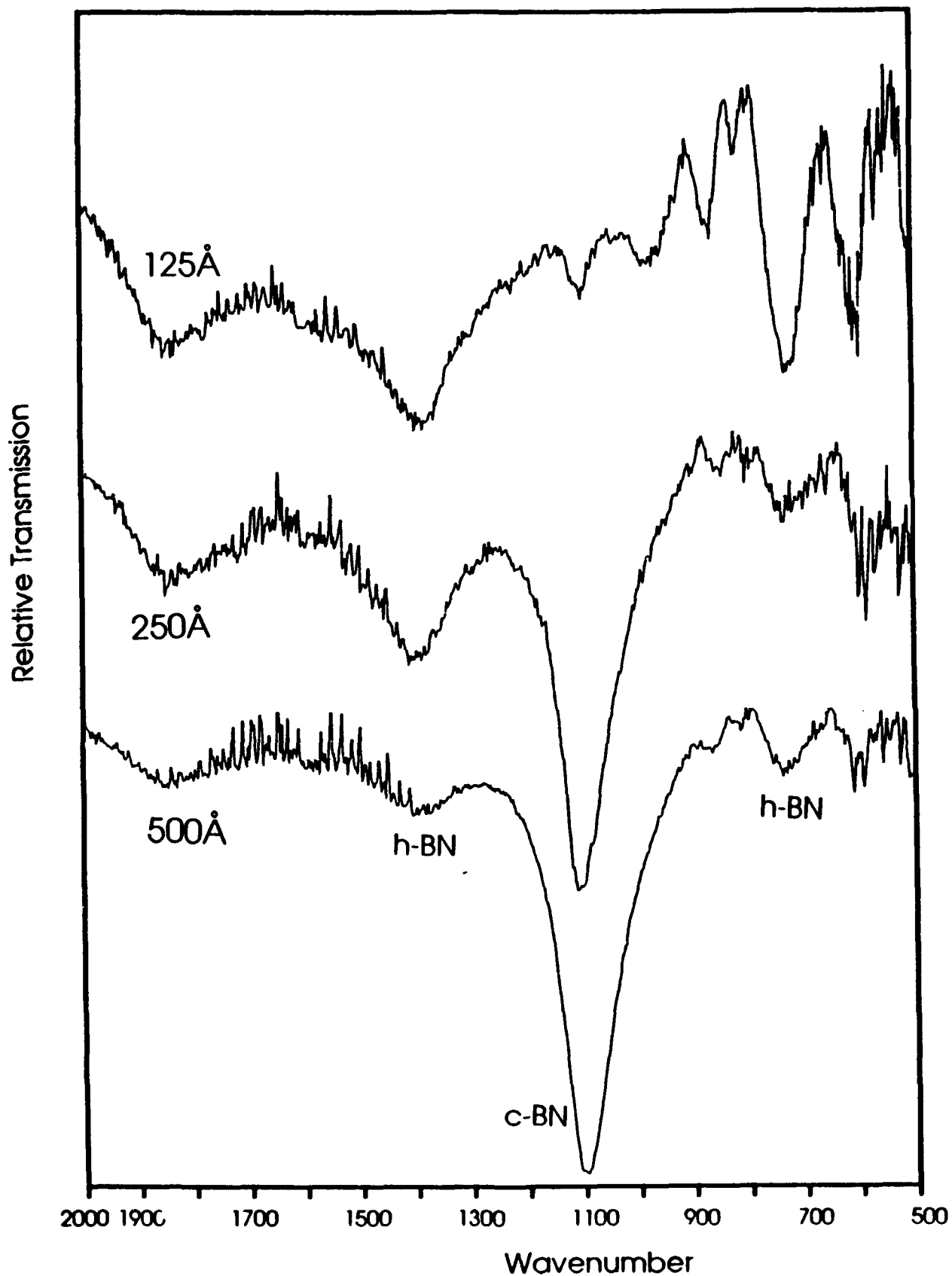


Figure 2. FTIR spectra of BN films of various thicknesses all deposited under the following conditions: Boron deposition rate: 0.25 Å/s; ion energy: 500 eV; ion flux: 0.12 mA/cm²; ion bombardment by 50:50 Ar:N₂; substrate temp: 400°C; substrate: 100 Si.

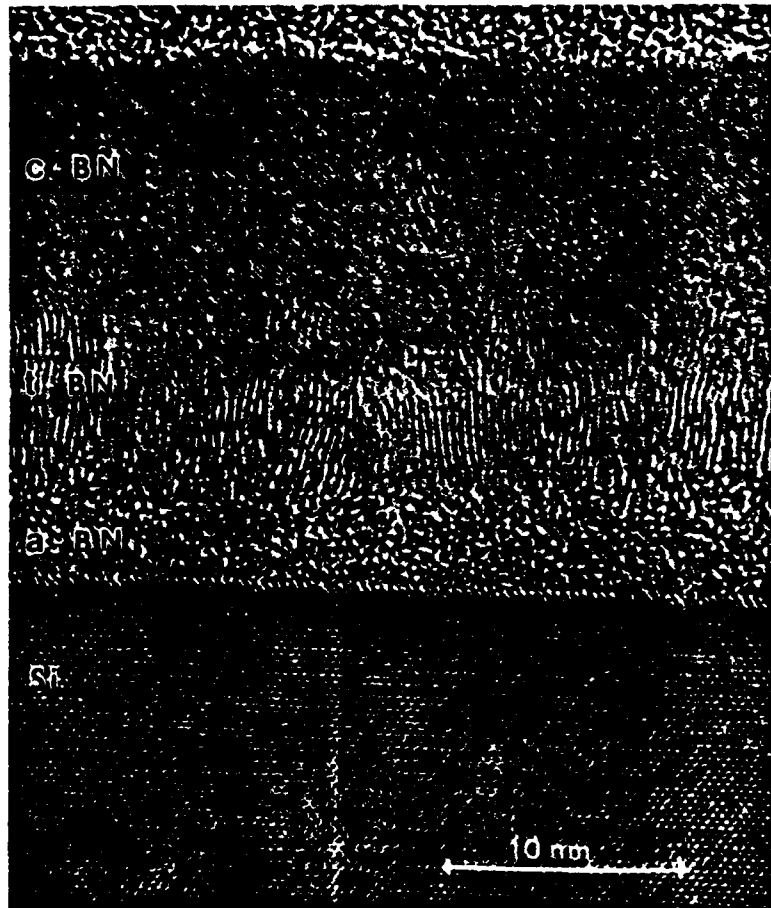
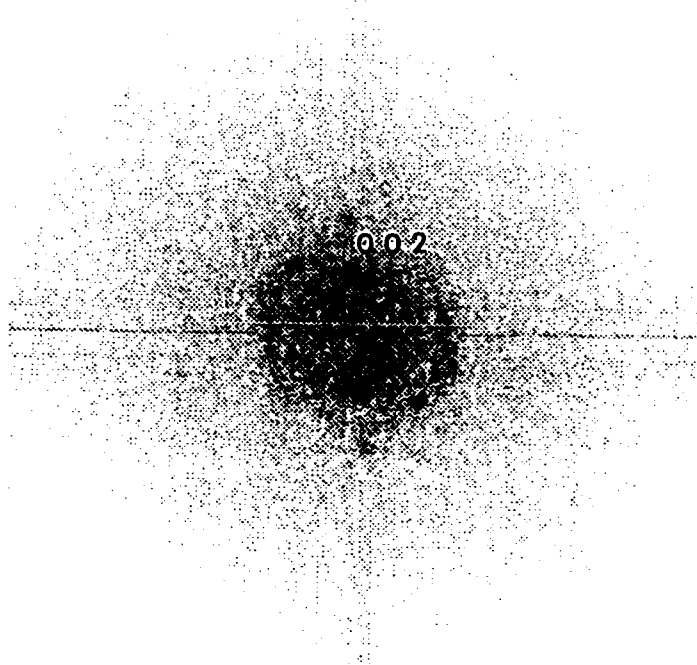


Figure 3. Cross-sectional HRTEM image of BN film showing Si substrate and regions of amorphous BN (a-BN), turbostratic BN (t-BN), and cubic boron nitride (c-BN).

a)



b)

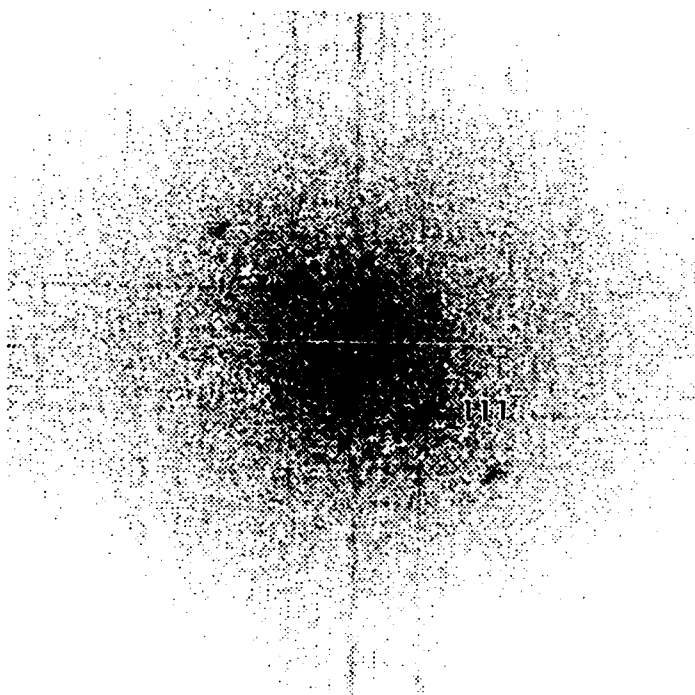


Figure 4. Fast Hartlee transform (FHT) patterns from the HRTEM image of Figure 3. (a) From the region labeled as t-BN. (b) From the region labeled as c-BN.

3. Effect of Substrate Temperature

Films were deposited at a range of substrate temperatures. It was found that increasing the deposition temperature from 300° to 400° to 500°C, while keeping other conditions constant, led to FTIR patterns with sharper cubic peaks, indicating an increase in grain size (Figure 5). The relative sizes of the cubic peaks as compared to the hexagonal peaks did not seem to change.

When depositing at temperatures of 600 and 700°C it was observed that at equal film thicknesses the films deposited at higher temperatures had a larger relative amount of hexagonal phase (Fig. 6). This would seem to indicate that the onset of the cubic layer occurs later.

4. Annealing

It has been found by most researchers that c-BN films grown on silicon crack and peel from the substrate due to intrinsic film stress. Methods of avoiding this have been studied, and generally consist of having some type of interface layer, for example an initial boron layer and gradually increasing the amount of nitrogen until stoichiometric boron nitride is reached. This method has been used together with a post-deposition anneal [4]. Another method involves high energy bombardment of the interface to get a mixed substrate-boron region [5]. These methods are useful for tribological applications. Their usefulness for electronic applications depends on the necessity for a particular application of having a sharp interface between the film and substrate. Fortunately, for many electronic applications it is possible to keep the film thickness at a level below which the adhesion problem occurs.

We have studied the effect of post-deposition annealing on deposited films. After deposition, substrates were moved, under vacuum, to a heating station where they were heated at 700°C for either 1 or 3 hours. It was found that while the annealing by itself did not completely prevent cracking and peeling, it did lessen and/or postpone it. On 500Å thick films the time until the initiation of peeling went from a few hours to one or two weeks. While still a problem, this delay in the onset of peeling is enough time to allow for film characterization to be performed on unpeeled films. It also appears that for very thin films (~250Å) the annealing may actually prevent the peeling.

5. Impurities

Rutherford backscattering was used to measure impurities in the films. It was found that films contained, in addition to boron and nitrogen, about 2 at.% argon, and ~0.1 at.% Ag and ~0.1 at.% W. The argon would be due to incorporation of bombarding argon ions. The silver is probably from the silver based paint used to hold down substrates and act as a heat conductor. The tungsten is from the neutralizer wire of the ion gun, through which the ion beam passes.

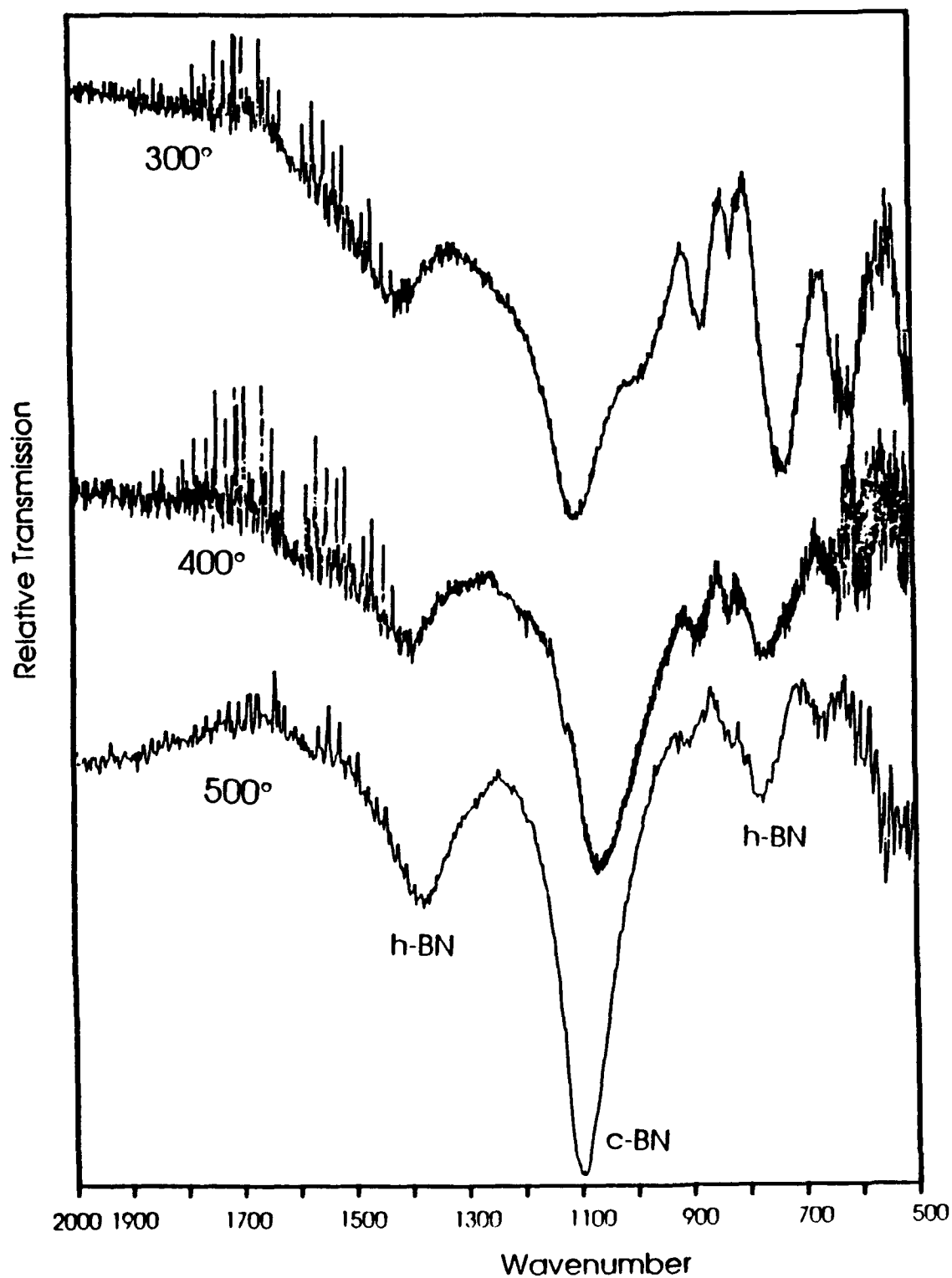


Figure 5. FTIR spectra of BN films deposited at different temperatures. Other deposition parameters were: Boron deposition rate: 0.25 Å/s; ion energy: 500 eV; ion flux: 0.14 mA/cm²; ion bombardment by 50:50 Ar:N₂; substrate temp: 400°C; film thickness: 250Å; substrate: 100 Si.

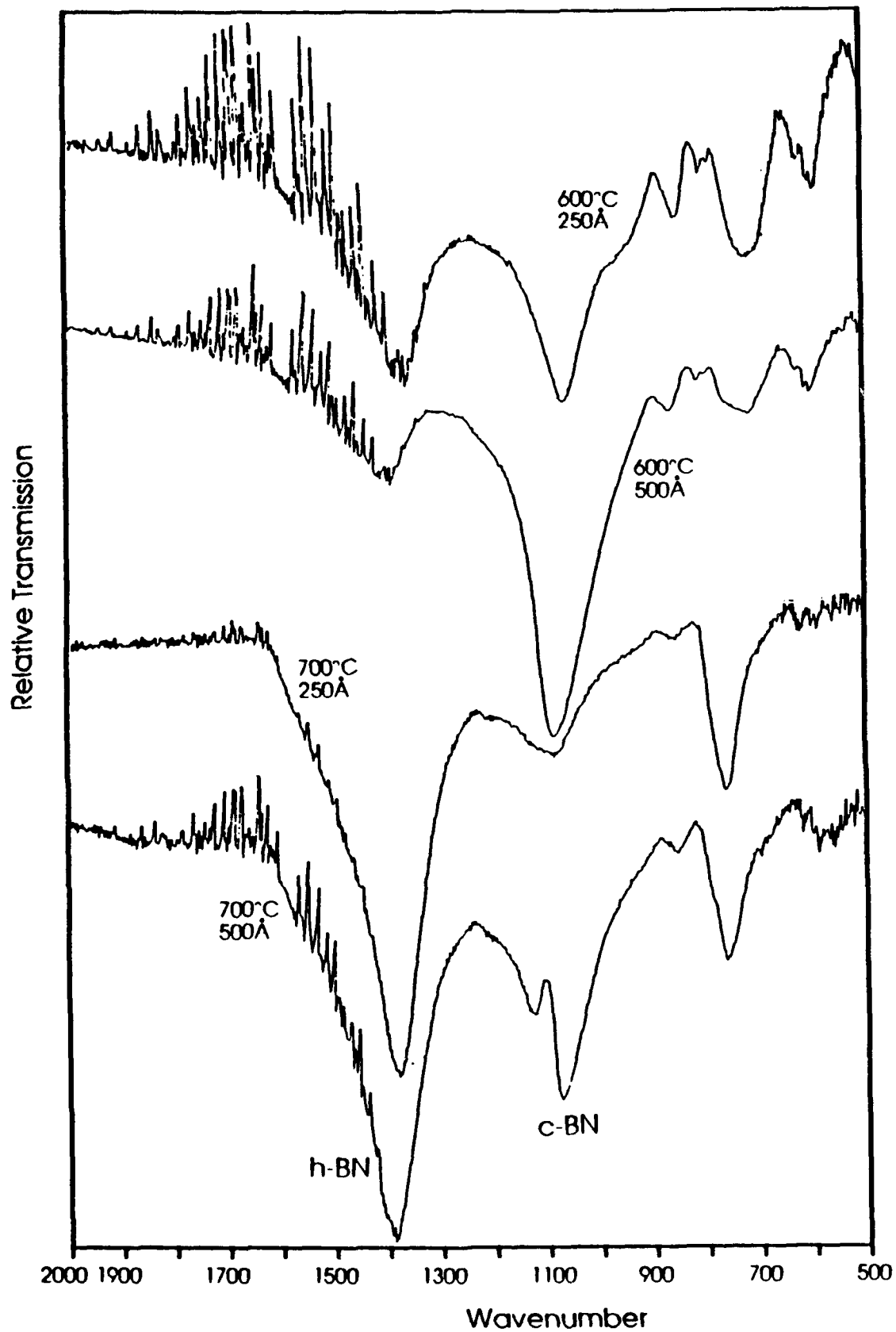


Figure 6. FTIR spectra of BN films deposited at different temperatures and thicknesses. Other deposition parameters were: Boron deposition rate: 0.5 Å/s; ion energy: 500 eV; ion flux: 0.24 mA/cm²; ion bombardment by 50:50 Ar:N₂; substrate: 100 Si.

6. Electrical

Electrical measurements (I-V) were done on a film using a mercury probe with a large and small area contact. The film was found to show rectifying behavior, being more conducting with a forward bias (Fig. 7). At present it is not clear how much of the current is actually carried through the BN film, and how much passes through the film to be carried through the Si substrate.

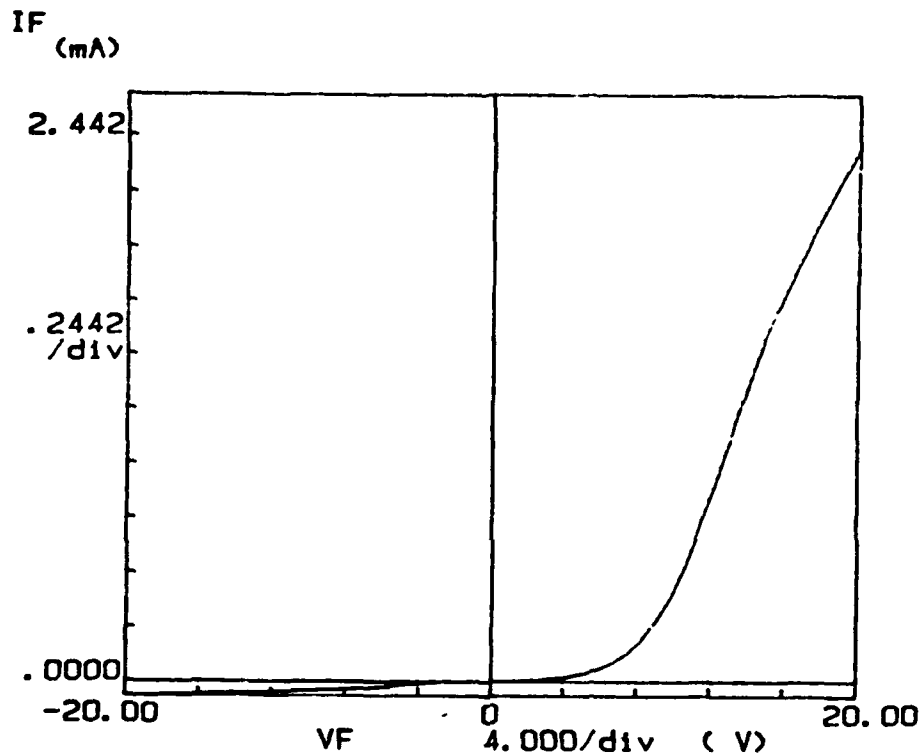


Figure 7. I-V curve for 250 Å film from Figure 2.

7. Diamond Substrates

Cubic boron nitride was deposited on diamond thin films on silicon substrates. The diamond films were grown using a microwave CVD process with 1% CH₄ and were 2-4 μm thick. Before the c-BN deposition the substrates with the diamond films were etched in a boiling H₂SO₄:HNO₃:HClO₄ solution in the ratio of 3:4:1 for 45 minutes to remove any graphite phase. 500 Å BN were then deposited on the diamond film. An FTIR spectrum for one of these films is shown in Figure 8. It is seen that the c-BN peak is present, and there is no evidence of an h-BN peak. Unfortunately the signal to noise ratio is very low, so the pattern is not very clear. This may be due to the small area of the substrates (~1 cm²). Depositions are presently being conducted on other diamond films, and we hope to get clearer results from those depositions.

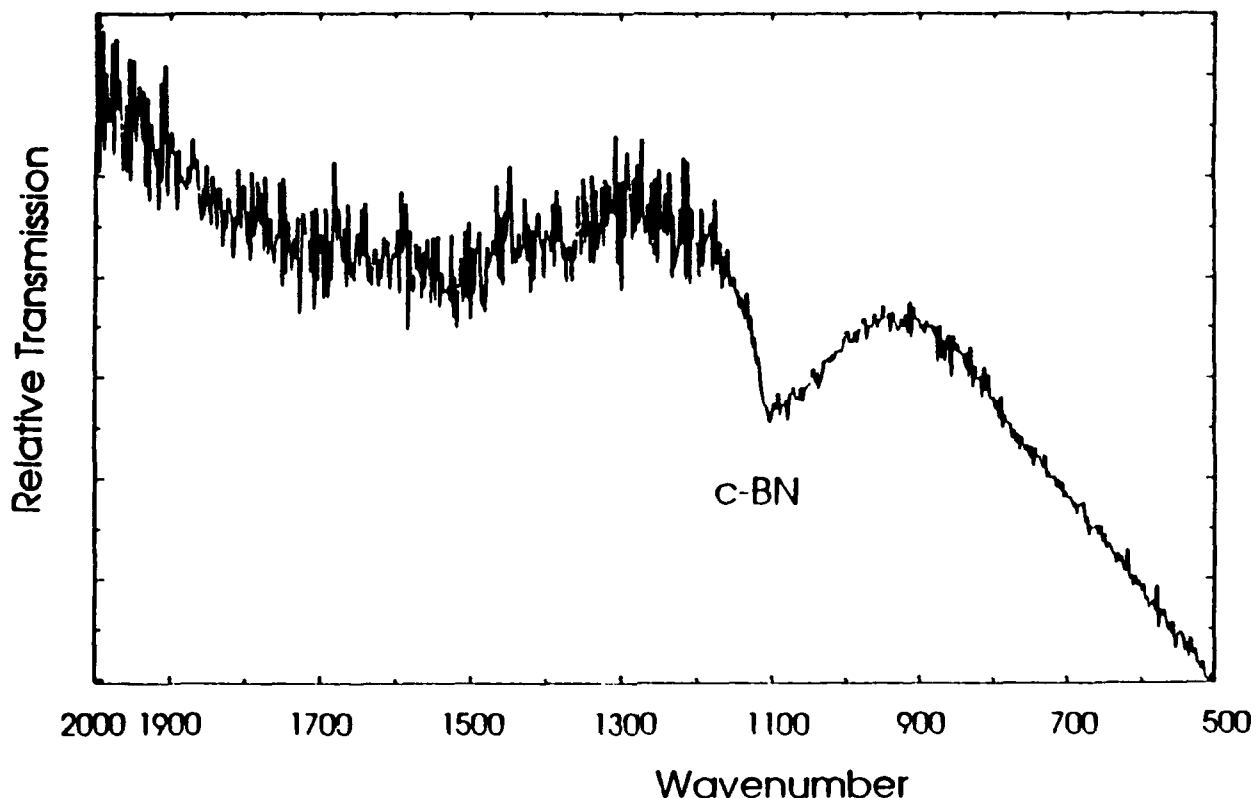


Figure 8. FTIR spectra of BN film deposited on diamond thin film on a silicon substrate. Deposition conditions: Boron deposition rate: 0.5 Å/s; ion energy: 500 eV; ion flux: 0.24 mA/cm²; ion bombardment by 50:50 Ar:N₂; substrate temp: 400°C; film thickness: 500Å.

D. Discussion

A major challenge in the growth of cubic boron nitride films has been maximizing the relative amount of cubic versus hexagonal phase. Growing 100% cubic films on Si has been exceedingly difficult. The best films we have deposited appear to be about 95% cubic, as determined by FTIR spectroscopy, which is among the highest purity reported. Having some hexagonal phase present in even the best films is typical for most reported results. This leads to the question of what causes the presence of the non-cubic boron nitride.

There are three possibilities as to what the 5% or more non-cubic BN is due to. One is that it is due to the grain boundary regions between regions of microcrystalline c-BN. A second possibility is separate h-BN (or t-BN) regions in the films. The results discussed above suggest a third possibility, that it may be due to layers of amorphous and hexagonal BN at the silicon surface that initially form before the growth of c-BN begins. The non-cubic BN present may also be due to a combination of these factors. It should be pointed out that the non-cubic forms of BN being discussed may more properly be referred to as sp² bonded BN to differentiate them from the sp³ bonded cubic form (and from the rare sp³ bonded wurtzitic hexagonal form), and can be either hexagonal, turbostratic, or amorphous BN. All

three will give the same basic FTIR spectra, with electron diffraction necessary to differentiate between them.

The HRTEM results we have shown, together with the FTIR results, show that, at least on silicon, interfacial layers develop which will lead to the characterization of films as partially hexagonal. These results are significant in that they explain why films grown on silicon always seem to have some hexagonal boron nitride component.

The results also show that the cubic layer, once it begins growing, is very pure. The initial non-cubic layers may be due to poor lattice matching between c-BN and silicon. The fact that the phase changes to cubic during growth is interesting because it suggests that at the deposition conditions used cubic may be the stable phase for boron nitride. The turbostratic phase would appear to be a non-stable phase forming only because of the influence of the Si substrate.

The results from the experiments on temperature effects indicate two things. First, that increased temperature leads to larger grain size. This conclusion is based on FTIR peak shapes and needs to be confirmed through TEM. If it turns out to be correct, it would indicate that the increased mobility brought about by the increase in surface temperature leads to the larger grain size. The second result from the temperature experiments is that the initiation of the cubic phase occurs later at higher temperatures. At this point it is unclear what would cause this effect. Again, TEM has not been performed on these high temperature depositions, once it is done it may provide useful information on the actual distribution of the phases.

Annealing appears to be a useful technique for lessening the stress in the films. Stress in thin films has two components, intrinsic and extrinsic stress. Extrinsic stress is due to differences in thermal expansion between substrates and film material. When the samples cool down after being deposited at an elevated temperature, the resulting difference in expansion will lead to a stress in the films. The intrinsic stress is a property of the film itself. It is typical for films subject to ion bombardment during deposition to develop a compressive intrinsic stress.

Annealing may relieve some of the intrinsic stress. On the other hand, due to the increased temperature cycling (from 400° to 700° to 20° instead of simply from 400° to 20°) it may actually increase the extrinsic stress if there is any reordering of the film atoms at 700°C.

The results from depositing on the diamond films indicate that cubic boron nitride will grow on diamond. The present thrust of our research is deposition on diamond, and optimizing the conditions for c-BN on diamond growth.

E. Conclusions

Cubic boron nitride thin films have been successfully grown on silicon using ion beam assisted deposition. The characterization results demonstrate that the films are predominantly

cubic, consisting of up to 95% cubic phase. We have found that on silicon the BN deposits with an initial amorphous layer of 50Å, followed by 70-100Å of turbostratic BN followed by cubic BN. This may explain why there always appears to be some non-cubic phase present in c-BN films. The effect of substrate temperature was studied, and it was found that increasing the temperature from 300° to 500° appears to increase the grain size. Depositions at higher temperatures (600° and 700°) appear to lead to an increase in the thickness of the non-cubic layer at the silicon interface. Depositions on diamond thin films have been done, and preliminary results show the growth of c-BN with little or no other phases present.

F. Future Research Plans/Goals

The goal of this research is to grow cubic boron nitride films of high enough quality that they may be used for electronic applications. Due to its properties including very high band gap and high thermal stability and thermal conductivity, cubic boron nitride has the potential of being an excellent material for high power and high temperature devices. To make c-BN films of electronic device quality will require several things. The first is an improvement in the relative phase ratio (cubic to non-cubic phases). Ideally, films would be 100% cubic.

A second requirement for electronic quality c-BN is to maximize grain size. Ideally this would mean single crystal films. Grain size needs to be maximized in order to minimize the area of grain boundaries which degrade the electrical properties of a film by acting as recombination sites, can be electrically active, are high diffusion paths, and are areas where concentrations of impurities may occur.

The third requirement is to minimize impurities in the films, which can act as scattering centers, and may be electrically active.

In order to maximize the percentage of cubic phase material in the film, it must first be determined whether the sp^2 material is due only to the interfacial layer at the silicon surface, or is also due to h-BN regions in the film or grain boundary regions (or some combination of these). This will be done using HRTEM characterization. If there is a significant amount of sp^2 material in the grain boundaries, then minimizing it will be a part of efforts to maximize grain size. If the main source is the interfacial region, then films will be grown on alternative substrates with better lattice matching, such as diamond. It may be possible that on diamond, c-BN growth will start immediately, with no intermediate h-BN layer. Both single crystal diamonds as well as diamond thin films will be used.

Increasing the grain size may be accomplished through varying the substrate temperature and/or the film growth rate. Changing the substrate temperature will change the atomic mobility of the depositing material. This may have an effect on both nucleation density and rate, and the crystallite growth rate. Changes in the film deposition rate may have similar effects on the film growth, with decreases in the rate having comparable effects to increasing

the substrate temperature. A third factor, the ion bombardment, also has a major effect on atomic mobility. The conditions which have been found to give the best c-BN films have been found by keeping the substrate temperature and film growth rate constant, and varying the ion bombardment flux. It may be that once the parameters that have been kept constant until now (temperature and growth rate) are varied, the optimal ion flux for getting c-BN will have changed. Therefore it is necessary to continue varying all three parameters. The limiting factor in increasing atomic mobility is that as it is increased resputtering of the deposited material may become a problem. This will have to be monitored. For determining grain size HRTEM will continue to be the primary characterization method.

In order to minimize impurities, the deposition procedures may need to be modified. Rutherford backscattering will continue to be used to measure impurities, due to giving a good depth profile of the impurity levels. XPS will also be used for compositional analysis. If silver continues to be found in the films, other methods of attaching the substrates, while still having good thermal conduction, will be tried. If tungsten is found to be a problem it may be possible to operate either without a ion neutralizer, or with a hollow cathode neutralizer, which eliminates the need for the tungsten filament.

Depositions will continue on diamond films. It is expected that diamond will be an excellent substrate for cubic boron nitride deposition due to the close lattice matching between diamond and c-BN, the good thermal expansion match, and the fact that diamond has a higher surface energy than c-BN. We have a broad range of diamond films available, deposited using various techniques from several sources. We will try to both optimize the conditions necessary for c-BN growth on diamond, as well as comparing the growth on diamond films prepared using different deposition conditions to see how that affects the c-BN growth.

As film quality improves, characterization emphasis will shift towards electrical measurements. As the deposition process is modified, with corresponding changes in film phase, grain size, and film impurity content, the effect on electrical properties will be closely monitored. Measurements will include I-V, C-V, 4-point probe, and Hall effect measurements.

G. References

1. J. Thomas, Jr., N. E. Weston, and T. E. O'Conner, *J. Am. Chem. Soc.* **84**, 4619 (1963).
2. R. H. Wentorf, Jr., *J. Chem. Phys.* **26**, 956 (1957).
3. F. Shimokawa, H. Kuwano, and K. Nagai, *Proc. 9th Symp. on ISLAT 85 Tokyo* (1985).
4. K. Inagawa, K. Watanabe, H. Ohsone, K. Saitoh, and A. Itoh, *J. Vac. Sci. Technol.* **A5**, 2696 (1987).
5. Y. Andoh, K. Ogata, and E. Kamijo, *Nucl. Instrum. Methods Phys. Res.* **B33**, 678 (1988).
6. M. Murakawa and S. Watanabe, *Surf. Coat. Technol.* **43/44**, 128 (1990).
7. H. Saitoh, T. Hirose, H. Matsui, Y. Hirotsu, and Y. Ichinose, *Surf. Coat. Technol.* **39/40**, 265 (1989).

8. R. Geick and C. H. Perry, *Phys. Rev.* **146**, 543 (1966).
9. P. J. Gielisse, S. S. Mitra, J. N. Plendl, R. D. Griffis, L. C. Mansur, R. Marshall, and E. A. Pascoe, *Phys. Rev.* **155**, 1039 (1967).
10. D. J. Kester, and R. Messier, to be published in *J. Appl. Phys.*, scheduled publication July 15, 1992.
11. Masao Murakawa, Shuichi Watanabe and Shojiro Miyake, *Diamond Films and Technol.* **1**, 55 (1991).
12. N. Yamashita, T. Wada, M. Ogawa, T. Kobayashi, H. Tsukamoto, and T. Rokkaku, presented at the ICMCTF-1992 meeting, San Diego, CA, 1992 (unpublished).

V. Deposition of Cubic Boron Nitride via Gas-Source Molecular Beam Epitaxy

A. Introduction

Boron nitride has long been known for its desirable properties as a highly insulating as well as a chemically and thermally stable material. The cubic phase of boron nitride was first reported by Wentorf,[1] who produced it in a high pressure apparatus and even made the initial measurements on the material's semiconducting properties. It has been used since then primarily for its high hardness in applications such as grinding and polishing. The cubic phase of BN is actually the zinc blende structure or in space group notation $F\bar{4}3m$ (Hermann-Mauguin) or T_d^2 (Schönflies). Boron nitride is very similar to carbon in that both exist in hexagonal, wurtzitic, and cubic forms and many of the properties in each of the phases are strikingly similar. The rare exception is that hexagonal boron nitride is an insulator and hexagonal carbon is a conductor. Among the many similarities include the fact that both diamond and c-BN are metastable under the conditions currently used for growth of thin films.

Interest in the cubic polymorph of BN as a semiconductor material has received much interest recently as a possible substrate for the deposition of diamond, due to the similar lattice parameters ($\Delta a_0=1.34\%$) and its wider bandgap which is in the range of 5.8–6.5 eV.[2, 3, 4] The very wide bandgap of c-BN also gives c-BN applications in its own right, as optical devices for the vacuum UV ($\lambda\sim 200$ nm). For a complete listing of materials-related properties of c-BN see *Landolt-Börnstein: Numerical Data and Functional Relationships in Science and Technology, Series III, Vols. 17 and 23*, or Ref. [5] (which also includes a side-by-side comparison of properties of c-BN with diamond).

Several approaches have been employed in the attempt to grow thin films of cubic boron nitride (c-BN). These include reactive diode[6] and rf sputtering,[7] ion implantation,[8, 9] plasma CVD,[10, 11, 12] microwave plasma CVD,[13, 14] and ion plating techniques.[15, 16, 17, 18] These attempts were successful in producing polycrystalline films of c-BN, predominantly of a mixed nature with both cubic and other phases present and of extremely fine grain size. It appears that most researchers succeeded in the deposition of c-BN if the technique included the input of additional energy from energetic ions during the deposition process.

Results from BN work undertaken in a cooperative effort with personnel at ASTeX, Inc., is not presented here, but instead, is appended as a preprint of a paper being submitted for publication. In addition, results on photo-activation effects on the growth and morphology of GaN is appended as a preprint of a paper also being submitted for publication.

B. Experimental Procedure

The primary deposition technique was GSMBE wherein elemental boron is evaporated from a high temperature effusion cell and molecular nitrogen gas is passed through a compact electron cyclotron resonance (ECR) plasma source to activate and dissociate the nitrogen. The growth system was a Perkin-Elmer 430 MBE system modified as described below. It consisted of three major sections: a load lock (base pressure $\approx 5 \times 10^{-8}$ Torr), a transfer tube (base pressure $\approx 3 \times 10^{-10}$ Torr) which was used to degas the substrates, and the growth chamber (base pressure $\approx 1 \times 10^{-10}$ Torr). The growth chamber was equipped with four standard 20 cc effusion cells that contained BN crucibles which were resistively heated with Ta wire heaters used in research of other nitrides.

One modification was the addition of a special high temperature effusion cell. This cell uses a W3%Re-W26%Re thermocouple and a tungsten alloy heater filament which is driven by a 2700 W DC power supply. It mounts on a standard 4.5" metal seal flange along with all the other metal evaporation sources. A BN crucible was used as it was believed that slight decomposition of the crucible at the elevated operating temperatures would not affect the growth of BN films. Prior to installation of the source, the BN crucible was loaded with 3 g of 99.9999% pure boron.

The more significant modification was the use of a compact ECR microwave glow-discharge plasma to dissociate/activate the N containing gas. This source was designed and commissioned in an in-house effort by Dr. Zlatko Sitar [1]. This source has the advantages of fitting inside the nominal two-inch diameter tube of the source flange cryoshroud and thus minimize the source to substrate distance. As a result, the flux of activated/dissociated species arriving at the substrate surface is increased. This source was attached in place of a more traditional effusion (or cracker) cell for the group V element. The nitrogen gas was taken from a bottle of compressed UHP-grade nitrogen, purified by a metallorganic resin bed gettering material and subsequently regulated to the source by a variable leak valve.

Substrate preparation involved a 30 min. exposure to UV which has been shown to remove hydrocarbon contamination [2], followed by a dilute acid etch to remove oxide layers. In the case of Si, a solution of H₂O:HF (10:1) was used [3], and for Cu, a solution of H₂O:HCl (10:1) was used [4]. Subsequently, the substrates were mounted on a Mo holder using either molten indium or silver paste. Silver paste was very important for the copper substrates as they were extremely sensitive to oxidation and would oxidize heavily in attempting to indium bond the substrates.

Samples were then loaded into a cryopumped load lock. After the initial evacuation, the samples were loaded into the transfer tube where they were degassed to a temperature of 700°C. Immediately after degassing they were loaded into the growth chamber and the deposition cycle began. Typical deposition conditions used are shown below in Table I.

Table I. Deposition Conditions used in GSMBE of BN.

Nitrogen pressure	$1-2 \times 10^{-4}$ Torr
Microwave power	20-50 W
Boron temperature	1725 - 1775°C
UV source power (where used)	500 W
Substrate temperature	400 - 500°C
Growth time (BN)	480 min.

The UV lamp, when used, was a 500 W high pressure Hg arc-lamp* with a collimating lens. The resulting spectral output is shown below in Figure 1. Note that the standard units for spectral irradiance are $\mu\text{W cm}^{-2} \text{nm}^{-1}$ and thus must be integrated to get power levels. This lamp was setup to illuminate the substrate surface from a sapphire viewport positioned normal to the growth surface. The sapphire composition permitted transmission of the entire range of UV wavelengths. Accounting for the mounting geometry and the various losses (including the sapphire window) resulted in an overall illumination power (for the spectrum 200-900 nm) of $\sim 0.5 \text{ W cm}^{-2}$.

This lamp was setup to illuminate the substrate surface from a sapphire viewport positioned normal to the growth surface. The sapphire window material permitted transmission of the entire range of UV wavelengths.

Subsequent to deposition the sample would either be moved to the load lock for removal from the system or transferred to the analytical system for additional characterization.

* Model 6285 lamp in #66042 housing, Oriel Corporation, Stratford, CT 06497

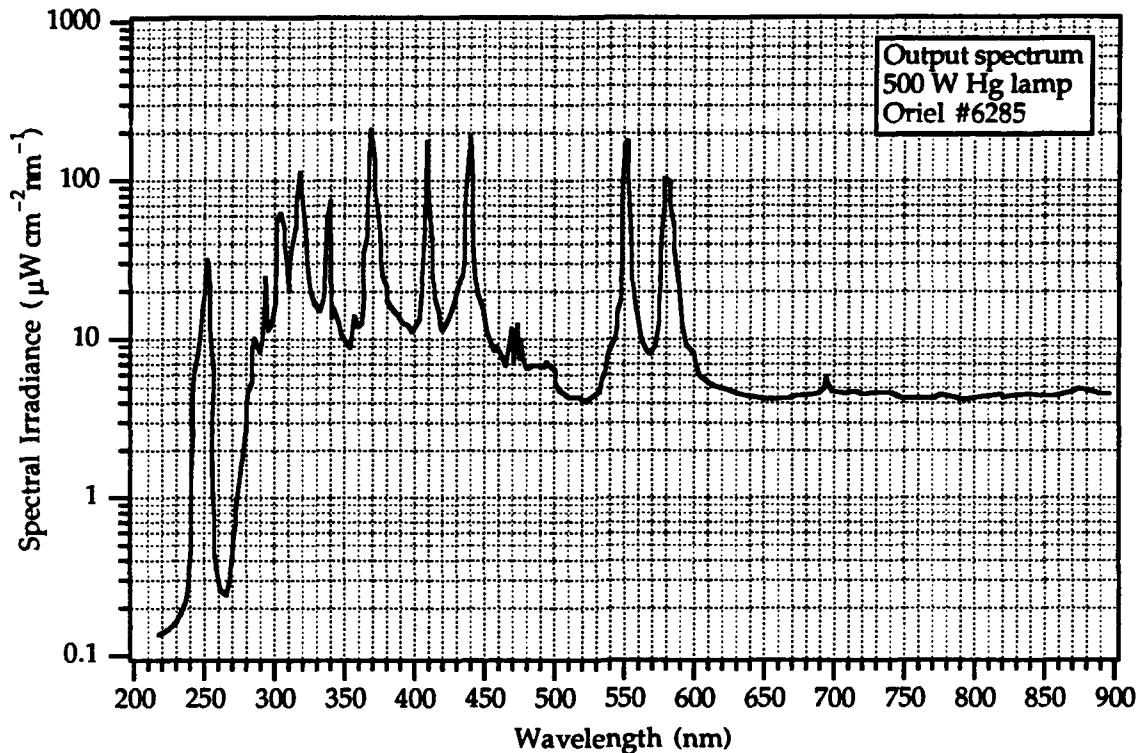


Figure 1. Spectral irradiance plot of the high pressure Hg arc lamp used for photo-enhanced deposition of BN films (After Oriel Corp. data for 500-W Hg-lamp).

C. Results

Shown in Figure 2 are the diffraction patterns from depositions at 500°C. Note that the sample with illumination fractured from handling which resulted in a high background at low angles due to the scattering from mounting clay. The spectrum shows only a broad band of reflections in the region of $<20-40^\circ$ (2θ), with the band from $<20-30^\circ$ being from the mount material. The origin of the broad band from $30-40^\circ$ is unclear, but does correspond to the forbidden c-BN (110) reflection. The Si (600) reflection was not observed on substrates without BN deposits. This reflection is exactly where the c-BN (400) reflection should be located due to the relative sizes of the unit cells ($\text{Si}/\text{c-BN}=1.5019$) and so was initially confused with the c-BN (400) reflection. This is an important point and so will be covered in detail in the Discussion.

Samples were next compared at a lower growth temperature to determine its impact on the phase formation. Figure 3 shows patterns from depositions at 400°C. The h-BN phase is apparently much more well crystallized at this lower temperature, based on the narrow line width of the h-BN (0002) peak. In both cases, the c-BN (400) peaks are present, but there is a dramatic decrease in the intensity of the h-BN (0002) peak for the illuminated case, indicating a strong inhibition of the formation of this phase.

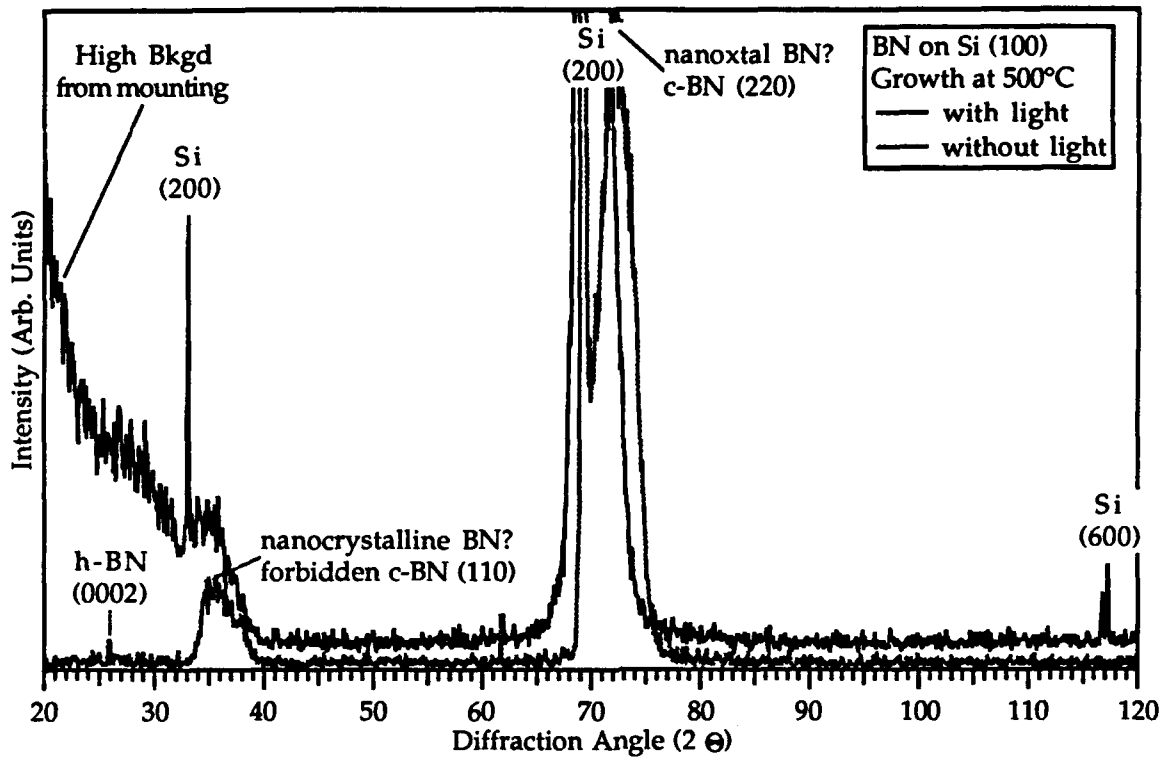


Figure 2. X-ray diffraction patterns (Cu K_{α} radiation) of BN deposited on Si (100) at 500°C with and without illumination from the Hg arc lamp.

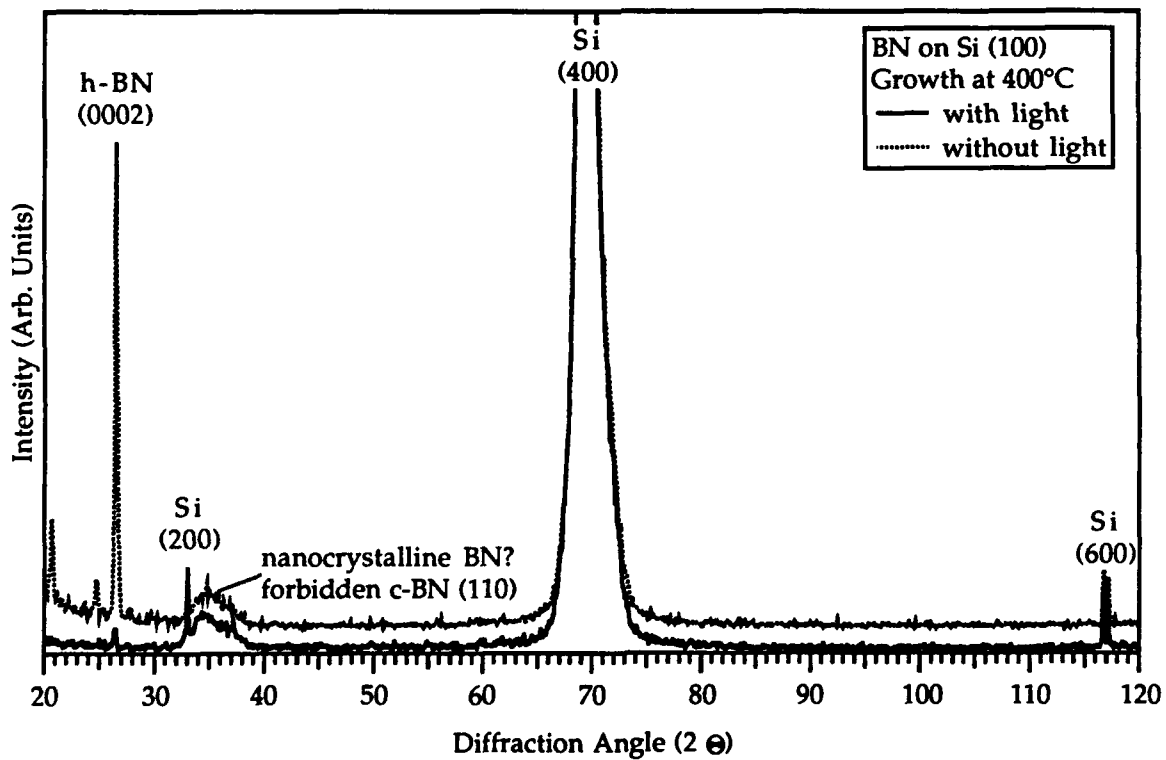


Figure 3. X-ray diffraction patterns (Cu K_{α} radiation) of BN deposited on Si (100) at 400°C with and without illumination from the Hg arc lamp.

Samples from a very long growth run (30 hrs.) at 500°C with illumination were prepared for cross-section high-resolution TEM. Stress in the film caused t regions to fracture away as they became thin, making observation extremely difficult. Thus photographic results will not be presented but will be discussed at the end of the next section.

D. Discussion

The results of the x-ray diffraction analyses described the interesting phenomenon of the superposition of the Si (600) and the c-BN (400) peaks, and there initial false assignment. This point will now be discussed further.

It is important to note that there is no c-BN (200) reflection, which should be present and an even stronger reflection than the c-BN (400) reflection (see Table II below). However, several researchers [5–12] did not observe the (200) predicted reflections in either of x-ray or electron diffraction patterns.

Table II. Observed diffraction peaks for c-BN standard using Cu K α radiation.
(Source: JCPDS card 35-1365 on CD-ROM)

Crystal Plane	Relative Intensity	Diffraction Angle	SAD Spacing ($\lambda L=2.15$ cm Å)
111	100%	43.3°	1.03 cm
200	5%	50.4°	1.19 cm
220	24%	74.1°	1.68 cm
311	8 %	89.9°	1.97 cm
400	2 %	116.9°	2.37 cm
331	3 %	136.4°	2.59 cm

In the case of electron diffraction patterns from polycrystalline material, one possible explanation for the missing (200) reflection is as follows. It is a moderately weak reflection (5%) and is located near (typically <2 mm) to the strongest reflection, and with the limited dynamic range of the film, the weak reflection is simply lost in the background [12]. For the cases of x-ray diffraction, the situation is more difficult to explain, as the angular separation is large (7° for Cu K α radiation), and modern detectors have extremely large dynamic range. However, in examining thin films, very often the major peaks are weak and broad, making secondary peaks difficult to resolve [6,7]. A second explanation, could be due to preferred orientation, or texturing, of the film [10]. This could cause peaks to appear weaker than they should from the JCPDS cards, which in turn would cause them not to be detected.

However, none of these explanations apply for the case where the (400) peak is observed [11]. Since the (200) peak is actually a stronger reflection, it is somewhat mysterious in its

absence. The explanation may lie in the origin of these two reflections. Standard texts on x-ray diffraction (e.g., *Elements of X-ray Diffraction, 2nd Ed.*, by B. D. Cullity, Addison-Wesley, 1978), give the scattering factors for the two peaks as: $F_{(200)}=4(f_N - f_B)$ and $F_{(400)}=4(f_N + f_B)$. From these equations one would assume that the (400) reflection would be stronger than the (200), but due to polarization and other factors, the intensity of higher angle peaks is reduced. The important point is that $F_{(200)}=4(f_N - f_B)$ is dependent on the difference of the atomic scattering factors. This fact permits two additional explanations for the lack of a (200) reflection: (a) nitrogen vacancies or boron interstitials, until the scattering factors were equivalent which would require deviations from stoichiometry of ~10%, or (b) a complete or partial disordering which would reduce the peak intensity below the detector limits. The former explanation should be observable from measurements of stoichiometry via techniques such as XPS, AES, or RBS. The latter explanation would require atomic level disorder in the lattice, though perhaps a sufficiently high concentration of microtwins and/or antiphase domain boundaries which would be observable via TEM and SAD.

One final point should be made regarding the presence of the forbidden Si (600) reflection only when a BN film is present. The explanation for this behavior is not clear at present but is probably some sort of stress-induced phenomenon.

Figure 2 showed that the addition of illumination did not dramatically affect the composition of the film beyond the appearance of the Si (600) which otherwise did not occur. Details of this possible effect will need to await further analysis. Figure 3 showed that the lowered growth temperature permitted h-BN to form, but then illumination during growth dramatically decreased the h-BN (0002) peak intensity.

Thus, while the crystallinity changes as indicated by x-ray diffraction, the bonding character in the larger volume of amorphous film is not dramatically affected. Deposition at 400°C involves a more dramatic change as evidenced by Figure 3.

High-resolution TEM examination of cross-section samples revealed an amorphous matrix, as would be expected from the x-ray and FT-IR (see annual progress report for 1991) analyses. Small regions of highly convoluted and distorted fringes corresponding to the h-BN (0002) were observed. This is probably indicative of the presence of a turbostratic structure, rather than a true hexagonal or graphitic one. Extremely small regions of mixed fringes were also observed, which may or may not correspond to c-BN were also observed. Further analysis is planned to clarify these observed structures.

E. Future Research

Experiments are planned to evaluate the spectral sensitivity of the observed behavior. By using band-pass filters, selected wavelengths can be removed from the illumination reaching the substrate. Thus questions regarding if above bandgap or below bandgap illumination are

dominant can be resolved. Beyond these experiments, future research in c-BN using the above GSMBE techniques is not warranted at present. The most fruitful direction for future research is the application of the photo-activation techniques discussed in this and previous reports to deposition technologies producing higher fractions of the c-BN phase.

F. References

1. R. H. Wentorf Jr., *J. Chem. Phys.* **36**, 1990 (1962).
2. R. M. Chrenko, *Solid State Commun.* **14**, 511 (1974).
3. C. Deshpandey and R. F. Bunshah, *Thin Solid Films* **163**, 131 (1988).
4. N. Miyata, K. Moriki, and O. Mishima, *Phys. Rev. B* **40**(17), 12028 (1989).
5. R. C. DeVries, *Cubic Boron Nitride: Handbook of Properties*, Technical Information Series, General Electric Company, Corporate Research and Development, 72CRD178, 1972.
6. K. H. Seidel, K. Reichelt, W. Schaal, and H. Dimigen, *Thin Solid Films* **151**(2), 243 (1987).
7. M. Mieno and T. Yoshida, *Jpn. J. Appl. Phys.* **29**(7), 1175 (1990).
8. M. Satou and F. Fujimoto, *Jpn. J. Appl. Phys.* **22**(3), L171 (1983).
9. Y. Andoh, *et al.*, *Nucl. Instrum. Meth. Phys. Res. B* **19/20**, 787 (1987).
10. J. Kouvetakis, V. V. Patel, C. W. Miller, and D. B. Beach, *J. Vac. Sci. Technol. A* **8**(6), 3929 (1990).
11. H. Saitoh, T. Hirose, H. Matsui, Y. Hirotsu, and Y. Ichinose, *Surf. Coat. Technol.* **39-40**(1-3), 265 (1989).
12. M. Okamoto, H. Yokoyama, and Y. Osaka, *Jpn. J. Appl. Phys.* **29**(5), 930 (1990).
13. A. Chayahara, H. Yokoyama, T. Imura, and Y. Osaka, *Appl. Surf. Sci.* **33/34**, 561 (1988).
14. O. Matsumoto, M. Sasaki, H. Suzuki, H. Seshimo, and H. Uyama, in *Tenth International Conference on Chemical Vapor Deposition*. G. W. Cullen, Eds. (The Electrochemical Society, Honolulu, Hawaii, 1987), pp. 552.
15. T. Ikeda, Y. Kawate, and Y. Hirai, *Kobelco Technol. Rev.* **6**, 1 (1989).
16. M. Murakawa and S. Watanabe, *Surf. Coatings Technol.* **43/44**(1-3), 128 (1990).
17. T. Nagatomo, Y. Hatooka, and O. Omoto, *Trans. IECE Jpn. E* **69**(4), 482 (1986).
18. T. Ikeda, Y. Kawate, and Y. Hirai, *J. Vac. Sci. Technol. A* **8**(4), 3168 (1990).
19. Z. Sitar, M. J. Paisley, D. K. Smith, and R. F. Davis, *Rev. Sci. Instrum.* **61**(9), 2407 (1990).
20. J. R. Vig, *J. Vac. Sci. Technol. A* **3**(3), 1027 (1985).
21. H. Lamb, personal communication, (1990).
22. I. Villegas, C. B. Ehlers, and J. L. Stickney, *J. Electrochem. Soc.* **137**(10), 3143 (1990).
23. O. Shanfield and R. Wolfson, *J. Vac. Sci. Technol. A* **1**(2), 323 (1983).
24. Y. Andoh, K. Ogata, and E. Kamijo, *Nucl. Instrum. Methods Phys. Res. B* **33**(1-4), 678 (1988).
25. K. Inagawa, K. Watanabe, K. Saitoh, Y. Yuchi, and A. Itoh, *New Diamond*, **60** (1988).
26. K. Inagawa, K. Watanabe, H. Ohson, K. Saitoh, and A. Itoh, *J. Vac. Sci. Technol. A* **5**(4), 2696 (1987).
27. S. Mineta, M. Kohata, N. Yasunaga, and Y. Kikuta, *Thin Solid Films* **189**(1), 125 (1990).
28. G. L. Doll, J. A. Sell, A. Wims, C. A. Taylor, and R. Clarke, in *Evolution of Thin-Film and Surface Microstructure Symposium*. C. V. Thompson, J. Y. Tsao, and D. J. Srolovitz, Eds. Boston, MA, 1990), pp. 333.
29. D. J. Kester, PhD (Pennsylvania State University, 1991).

VI. Impurity Doping and Contact Formation in AlN and GaN

A. Introduction

The III-V nitrides have long been known to possess properties that have potentially great technological value. These materials can be considered as largely covalent ceramics, whose unique combination of properties are only beginning to be put to use. Aluminum nitride, especially, exhibits great thermal stability, high radiation resistance, high thermal and acoustic conductivity, and a thermal expansion coefficient comparable to that of silicon.

For electronic and optoelectronic device applications, however, the most important characteristics of the III-V nitrides are that they are all semiconductors having wide, direct band gaps and form complete solid solutions with one another. With the band gap of GaN being 3.4 eV and that of AlN 6.2 eV, the possibility exists for optical and optoelectronic devices active from the blue region of electromagnetic spectrum to well into the ultraviolet. To date, semiconductor devices have been developed that operate in the infrared to green regions of the spectrum, but as yet attempts to push this capability to shorter wavelengths have been unsuccessful. The present study is part of an effort to characterize the semiconductor and optical properties of the III-V nitrides, and to demonstrate the valuable technological capabilities of these materials.

B. Proposed Experimental Procedure

1. Impurity Doping of AlN and GaN

General Considerations. In order to create logic devices and optoelectronic devices such as light-emitting diodes (LEDs) and heterostructure lasers from AlN and GaN, it must be possible to engineer the materials' electrical properties so as to allow both p- and n-type conductivity. However, as noted by Neumark [1], the goal of good bipolar conductivity in wide band gap semiconductors has been elusive for many years. Difficulties in achieving p-type conductivity, especially, have been attributed by many to compensation of the charge carriers by native defects -- especially N vacancies, in GaN and InN -- and by the amphoteric nature of some impurities (i.e., some impurities do not occupy the appropriate lattice site to function as active dopants) [1-4]. Neumark *et al.* [1,2] point out that, fundamentally, an impurity's lack of solubility in a semiconductor is the reason behind the difficulty in activating the impurity as a dopant. However, at the present time detailed knowledge of impurity solubilities in these materials is not available. In any case it may be necessary to incorporate non-equilibrium amounts of impurities in order to obtain significant conductivity.

A systematic investigation of both p- and n-type impurity doping in AlN has not been performed to date; the present study is an attempt to establish a basic understanding of the most likely donor and acceptor candidates. In making choices for electrically active donor

and acceptor impurity candidates, the results of previous studies provide a number of useful guidelines. Investigations of AlN in the early 1960s indicated that the presence of the isomorphous impurity Al_2O_3 caused p-type conductivity, lowered the overall resistivity of AlN from 10^{11} - 10^{13} $\Omega\text{-cm}$ to 10^3 - 10^5 $\Omega\text{-cm}$, and created an electronic transition that gave the material a blue color and had a thermal activation energy of 1.4 ± 0.06 eV [5,9,10]. More recent work has shown that the native defects in AlN and its most common impurities—specifically, oxygen and carbon—create states deep within the band gap that act as traps for the charge carriers, and do not result in useful p- or n-type conductivity [6-8].

More progress has already been made with the development of GaN as a wide band gap semiconductor than with AlN. Most of the GaN crystals grown to date exhibit n-type conductivity which has generally been attributed to N vacancy states. Obtaining p-type conductivity from GaN has been much more challenging, and only recently has some success been achieved. Silicon has recently been found to be an effective donor in both GaN and $\text{Al}_x\text{Ga}_{1-x}\text{N}$ alloys, when grown into the films by metalorganic vapor phase epitaxy (MOVPE) [4,11]. Spectroscopic and electrical analysis indicate that the Si impurity creates a shallow donor level near the band edge and occupies the group III site (Al or Ga) in the lattice.

Amano *et al.* [12,13] succeeded in obtaining p-type conductivity and consequently a blue LED p-n junction by exposing Mg-doped GaN to low-energy electron beam irradiation (LEEBI). Soon afterwards, Amano *et al.* also observed near-UV stimulated emission from GaN at room temperature [14]. The success of the LEEBI treatment has produced intriguing results; however, the mechanism of the dopant activation is not yet understood, and from a practical device-manufacture standpoint the electron beam treatment is not an attractive solution because the process is time-consuming and serial in nature.

The general rule followed in the field of impurity doping is that the impurity atom valence $Z_i = Z_s \pm 1$, where Z_s is the valence of the semiconductor matrix atom. In planning the present study, the investigators have based their choices for dopant candidates on the likelihood of the impurity atom occupying the appropriate nitride lattice site. This likelihood is estimated on the basis of compatibility of covalent radii and on the known or suspected chemical reactivity of the impurity with either element in the crystal. Both AlN and GaN films will be grown using molecular beam epitaxy (MBE), and it is planned to incorporate the following elements via ion implantation: Si and Ge as donor impurities, and Be, Mg, Zn and C as acceptor dopants. After implantation, the samples will be characterized as described below.

Ion Implantation. Over the past 20 years, ion implantation has become the method of choice for selective impurity doping in the fabrication of integrated circuits [15]. As pointed out by Pankove and Hutchby [16], ion implantation is the most reliable method of incorporating a known concentration of a spectroscopically pure element into a solid. Ion

implantation is a relatively straightforward process, the technology for which by now has been refined and well established. One drawback of the procedure is the significant amount of damage that can be induced in the target material by the high-energy bombardment of ions. This lattice damage is dependent on the ion beam energy and the mass of the incident particles, and can involve defects that affect the electronic behavior of the crystal.

In the present study, both p- and n-type dopants will be implanted into AlN and GaN. The implantation will be conducted at elevated temperature (500°C) in order to provide some opportunity for lattice repair during the implantation process. Previous studies with another refractory, wide band gap compound semiconductor, SiC [17], revealed that implantation at high temperature produced an *in situ* annealing effect that greatly improved the activation of both p- and n-type dopants. A neutral species, Ar, will also be implanted under similar conditions to provide a non-electrically active control comparison for the characterization of implantation-induced defects. Two different total impurity doses will be incorporated ($N=10^{17}$ and 10^{18} cm⁻³) and the beam energy will be varied to maintain a similar doping profile. Theoretical implantation profiles will be calculated using the TRIM program developed by J. F. Ziegler and J. P. Biersack [18]. Actual implantation profiles of both composition and target damage will be characterized by means of Rutherford Backscattering Spectroscopy (RBS) and secondary ion mass spectroscopy (SIMS).

Characterization. Hall effect measurements, current-voltage (I-V) measurements, and capacitance-voltage (C-V) measurements will be used to characterize the electrical behavior of the ion-implanted nitrides over a wide range of temperatures. Photoluminescence (PL) and cathodoluminescence (CL) will be used to investigate the materials' spectroscopic properties and energy level structure. Post-implantation annealing treatments will be performed to study the effect of further thermal exposure on the activation of the dopants. Control samples consisting of pure, as-grown AlN and GaN films will be exposed to the same heat-treatment schedule as the ion-implanted specimens for comparison.

2. Electrical Contacts to AlN and GaN

Choices for Metal Contacts. In order to take full advantage of the properties of a semiconductor and connect it to other components, it must be possible to make both ohmic and rectifying (Schottky) contacts to the material with appropriate conductors, usually metals. For the compound semiconductors, the art of perfecting the properties of both types of interfaces has been found to be a challenging one. It has become plain that there are many factors, especially interface reaction chemistry and morphology, that significantly affect the nature and behavior of contacts. Many of these factors are only beginning to be understood and documented.

The physical condition that determines the nature of an electronic interface is the Fermi level. From an ideal electronic standpoint, ignoring the existence of interfacial electron states, the nature of a solid state junction is determined by the difference in work function (or, by the same token, electron affinity) of the two materials. Since the Fermi levels of the two materials must align at equilibrium, the junction barrier height E_b can be expressed using the following relationship:

$$E_b = (E_g - E_{fs}) + (\phi_m - \phi_s)$$

where E_g is the semiconductor band gap, E_{fs} is the semiconductor Fermi level with respect to the top of the valence band, and ϕ_m and ϕ_s are the work functions of the metal and semiconductor, respectively. According to this simple model, if the semiconductor is n-type then $\phi_m < \phi_s$ produces an ohmic contact and $\phi_m > \phi_s$ produces a rectifying contact; the reverse is true for a p-type semiconductor. Rhoderick [19] points out that ohmic contacts are uncommon in practice and the majority of metal-semiconductor combinations produce rectifying contacts.

Experimentally it is found that the barrier height for a given interface is not very dependent on the choice of metal. The presence of additional electron states at the interface can significantly change the junction's electron energy structure; the origins of and mechanisms behind these states are not yet completely understood. It has been observed that improving the chemical and morphological abruptness of an interface and making a close match of thermal and mechanical properties is helpful for improving the performance of rectifying contacts. By the same token, extending a gradation of composition and properties at the interface generally improves ohmic contacts.

Contact Candidates. The first set of ion-implanted AlN and GaN specimens will be used in an effort to form ohmic contacts to the doped materials. Aluminum nitride has a relatively high work function at $\phi_{AlN} = 5.35$ eV [20]; that of GaN is not well established at this time. According to the simple Schottky-Mott-Bardeen model, the work function of the metal must be higher than 5.35 eV in order to form an ohmic contact with p-type AlN. Only two metals comfortably satisfy this condition: Se ($\phi_{Se} = 5.9$ eV) and Pt ($\phi_{Pt} = 5.65$ eV). Platinum is the more attractive choice because of its chemically noble and refractory character. Gold also has a relatively high work function ($\phi_{Au} = 5.1$ eV; $\phi_{Au(111)} = 5.31$ eV) and is noble and refractory. Both Pt and Au form several compounds with both Al and Ga, but do not react appreciably with N.

As ohmic contact materials for p-type nitrides, Al, Ga and In suggest themselves because of their uncomplicated chemical relationships with their nitrides and their relatively low work functions. Table I lists some of the relevant physical properties of the chosen contact metals. The metal layers will be deposited *in situ* on the as-grown surface of the AlN and GaN in order to minimize chemical complications at the interface and, in the case of AlN, to serve as

a protective layer on the nitride. Aluminum nitride reacts readily with atmospheric oxygen and moisture to form an adherent, passive oxide film which creates an insulating barrier on the AlN surface. For these reasons, ion implantation will be performed through the metal contact films.

Table I. AlN/GaN Ohmic Contact Candidates

	AlN	GaN	Pt	Au	Al	Ga	In
structure	wurtzite	wurtzite	fcc	fcc	fcc	orth.	tetr.
lattice parameter	a: 3.11 c: 4.98	a: 3.189 c: 5.185	3.9240 2.7747*	4.0786 2.8840*	4.0497 2.8636*	2.484*	3.2513*
m.p.(°C)	3000**	800**	1772	1064	660	30	157
resistivity (RT) (Ω-cm)	1000 and up	high	low	low	low	low	low
work function (eV)	5.35	?	5.65	5.1(+)	4.28	4.2	4.12
surface energy (mJ/m²)	990±110	?	2691	1626	1085	720	591
thermal exp. coeff. (RT) (10⁻⁶ 1/K)	5.27 4.15	5.59 3.17	9.	14.2	25.	?	?
thermal conduct. (W/cm·K)	2.	1.3	20.73	3.15	2.37	?	?

* Nearest neighbor distance (a-plane for hexagonal; (111) for fcc)

** Approximate decomposition temperature; depends on atmosphere, pressure, etc.

Characterization. Current-voltage measurements will be conducted to study the basic electrical behavior of the contacts. Transmission electron microscopy (TEM), particularly of cross-sectional specimens, will be used to characterize the physical structure of the interfaces. The feasibility of using scanning tunneling spectroscopy (STS) and ballistic electron emission microscopy (BEEM) to study the electronic structure and I-V character of the contacts will be investigated. Ballistic electron emission microscopy is a potentially valuable technique for the spectroscopic investigation of subsurface electronic structure and is a

variation on the basic scanning tunneling microscopy procedure. Both BEEM and STS have been used to investigate compound semiconductors and their interfaces with metals [21-26].

C. Summary

The III-V nitrides are a family of materials that are likely to have great value in the areas of electronic and optoelectronic device development. Their wide, direct band gaps give them the potential for optical activity at shorter wavelengths than has been achieved to date with other materials. The present study is a systematic investigation of the issues of p- and n-type impurity doping and electrical contact formation in AlN and GaN. It is hoped that the results of this effort will contribute to a breakthrough in the practical utilization of these promising materials.

D. References

1. G.F. Neumark, Phys. Rev. Lett. **62**, 1800 (1989).
2. D.B. Laks, C.G. Van de Walle, G.F. Neumark, S.T. Pantelides, Phys. Rev. Lett. **66**, 648 (1991).
3. J. Ren, K.A. Bowers, B. Sneed, D.L. Dreyfus, J.W. Cook, Jr., J.F. Schetzina, R.M. Kolbas, Appl. Phys. Lett. **57**, 1901 (1990).
4. N. Koide, H. Kato, M. Sassa, S. Yamasaki, K. Manabe, M. Hashimoto, H. Amano, K. Hiramatsu, I. Akasaki, J. Cryst. Growth **115**, 639 (1991).
5. J. Edwards, K. Kawabe, G. Stevens, R.H. Tredgold, Solid State Commun. **3**, 99 (1965).
6. V.F. Veselov, A.V. Dobrynin, G.A. Naida, P.A. Pundur, É.A. Slotsenietse, E.B. Sokolov, Inorganic Materials **25**, 1250 (1989).
7. J.H. Harris, R.A. Youngman, R.G. Teller, J. Mater. Res. **5**, 1763 (1990).
8. R.A. Youngman, J.H. Harris, J. Am. Ceram. Soc. **73**, 3238 (1990).
9. G. Long, L.M. Foster, J. Am. Ceram. Soc. **42**, 53 (1959).
10. K.M. Taylor, C. Lennie, J. Electrochem. Soc. **107**, 308 (1960).
11. H. Murakami, T. Asahi, H. Amano, K. Hiramatsu, N. Sawaki, I. Akasaki, J. Cryst. Growth **115**, 648 (1991).
12. H. Amano, I. Akasaki, T. Kozawa, K. Hiramatsu, N. Sawaki, K. Ikeda, Y. Ishii, J. Luminescence **40&41**, 121 (1988).
13. H. Amano, M. Kito, K. Hiramatsu, I. Akasaki, Japan. J. Appl. Phys. **28**, L2112 (1989).
14. H. Amano, T. Asahi, I. Akasaki, Japan. J. Appl. Phys. **28**, L150 (1990).
15. M.D. Giles, in *VLSI Technology*, 2nd ed. (McGraw-Hill, New York, 1988) p. 327.
16. J.I. Pankove, J.A. Hutchby, J. Appl. Phys. **47**, 5387 (1976).
17. J.A. Edmond, S.P. Withrow, W. Wadlin, and R.F. Davis in *Interfaces, Superlattices and Thin Films*, edited by J.D. Dow and I.K. Schuller (Mater. Res. Soc. Proc. **77**, Pittsburgh, PA 1987) p. 193.
18. J.F. Ziegler and J.P. Biersack, *The Stopping and Range of Ions in Solids* (Pergamon, New York, 1985).
19. E.H. Rhoderick, *Metal-Semiconductor Contacts* (Oxford University Press, New York, 1988) pp. 14-15.
20. J. Pelletier, D. Gervais, C. Pomot, J. Appl. Phys. **55**, 994 (1984).
21. W.J. Kaiser and L.D. Bell, Phys. Rev. Lett. **60**, 1406 (1988).
22. A.E. Fowell, R.H. Williams, B.E. Richardson, A.A. Cafolla, D.I. Westwood, D.A. Woolf, J. Vac. Sci. Technol. B **9**, 581 (1991).
23. M. Prietsch and R. Ludeke, Phys. Rev. Lett. **66**, 2511 (1991).
24. G.S. Rohrer and D.A. Bonnell, J. Am. Ceram. Soc. **73**, 3257 (1990).
25. R.M. Feenstra and P. Mårtensson, Phys. Rev. Lett. **61**, 447 (1988).

VII. Development of Ultra-violet-Visible Luminescence Facility

A. Introduction

Luminescence is the emission of photons due to excited electrons in the conduction band decaying to their original energy levels in the valance band. The wavelength of the emitted light is directly related to the energy of the transition, by $E=hn$. Thus, the energy levels of a semiconductor, including radiative transitions between the conduction band, valance band, and exciton, donor, and acceptor levels, can be measured [1,2].

In luminescence spectroscopy various methods exist to excite the electrons, including photoluminescence (photon excitation), and cathodoluminescence (electron-beam excitation). In each technique signal intensity is measured at specific wavelength intervals using a monochrometer and a detector. The intensity versus wavelength (or energy) plot can then be used to identify the characteristic energy band gap and exciton levels (Intrinsic luminescence) of the semiconductor, and the defect energy levels (extrinsic luminescence) within the gap [1].

Both photo- and cathodoluminescence analysis has been performed on AlN, GaN, and $Al_xGa_{1-x}N$ semiconductors [3-8]. Much of the work has been in measuring the low temperature GaN luminescence peaks. Work on AlN has been limited by the energy gap of 6.2 eV, which corresponds to a wavelength (200 nm) that is lower than most of the optical light sources. An excimer laser using the ArF line (193 nm) can be used, but caution must be taken when operating at these wavelengths.

Few time-resolved luminescence measurements have been performed on AlN and GaN. In a time-resolved measurement a pulsed source is used to excite the sample, and the luminescence is measured at short sampling intervals after the pulse. The result is an intensity vs. time plot. Time resolved spectroscopy is useful for separating the emission bands of the investigated samples with different decay times. It is often used to measure donor-acceptor recombination rates and minority carrier lifetimes [1].

Depth-resolved information can be obtained using cathodoluminescence, since generation depth varies with beam voltage. This technique is particularly useful for studying ion implanted semiconductors and layered structures [1].

B. Future Research Plans/Goals

A combined photo- and cathodoluminescence system is currently being assembled. It will include three optical sources and a beam blanking electron gun. The sample will be in a UHV chamber, and the monochrometer and collection optics will be in a vacuum environment. The optical sources include a pulsed excimer laser, which can operate at wavelengths of 193 nm (6.4 eV), 248 nm (5.0 eV), and 308 nm (4.0 eV); it can be used to

measure the luminescence of AlN. A CW He-Cd laser, which operates at wavelengths of 325 nm and 442 nm, and a xenon arc lamp are the other two light sources. The xenon lamp, which has continuous emission through the UV/Vis range, will be used with a small monochromator to select a single wavelength of excitation.

The beam blanking capability of the electron gun will make it possible to do time-delay studies of the semiconductors. With a maximum beam voltage of 15 keV it will also be possible to perform depth-resolved spectroscopy.

Cathodoluminescence in the TEM will also be performed on the nitride films through a collaboration with Dr. Roger Graham at Arizona State University. In the TEM environment the luminescence from individual defects can be examined, and hence the source of extrinsic luminescence peaks can be identified.

The optical properties of the nitride films will be examined through a collaboration with Dr. Roger H. French of Du Pont. Reflectance and transmission measurements in the visible to the vacuum ultraviolet light range ($E \geq 40$ eV) are possible. Optical transmission measurements probe the fundamental absorption edge and determine the optical band gap energy. Reflectance measurements are useful for probing interband transitions lying at higher energies, where the material is opaque. Reflectance measurements also probe many-body excitations, such as exciton, and provide a valuable probe into how the electrons and holes interact in the lattice. VUV spectroscopy over a wide range (5 to 40 eV) allows one to exhaust the transitions of the intrinsic electronic structure and to determine the high-frequency dielectric constant and optical properties from Kramers-Kronig analysis. This provides a quantitative electronic structure information.[9] VUV spectroscopy has been performed on single crystal and polycrystalline AlN, but little has been done on AlN or GaN thin films [10].

C. References

1. B. G. Yacobi and D. B. Holt, *Cathodoluminescence Microscopy of Inorganic Solids*, Plenum Press, New York (1990)
2. Micheal D. Lumb, Ed., *Luminescence Spectroscopy*, Academic Press, New York (1978)
3. S. Strite and H. Morkoç, GaN, AlN, and InN Review.
4. R. A. Youngman and J. H. Harris, *J. Am. Ceram. Soc.*, **73** [11] 3238 (1990)
5. S. Strite, J. Ruan, Z. Li, N Manning, A. Salvador, H. Chen, D. J. Smith, W. J. Choyke, and H. Morkoç, "An investigation of the properties of b-GaN grown on GaAs."
6. M. A. Khan, R. A. Skogman, J. M. Van Hove, S. Krishnankutty, and R. M. Kolbas, *Appl. Phys. Lett.* **56** (13) 1257 (1990)
7. Z. Sitar, M. J. Paisley, J. Ruan, J. W. Choyke, and R. F. Davis.
8. V. F. Veselov, A. V. Dobrynin, G. A. Naida, P. A. Pundur, E. A. Slotsenietse, and E. B. Sokolov, *Inorganic Materials*, **25** (9) 1250 (1989)
9. R. H. French, *J. Am. Ceram. Soc.*, **73** [3] 477 (1990)
10. R. H. French and Steven Loughlin, Private Communication.

VIII. Distribution List

	Number of Copies
Mr. Max Yoder Office of Naval Research Electronics Division, Code: 1114SS 800 N. Quincy Street Arlington, VA 22217-5000	2
Administrative Contracting Officer Office of Naval Research Resident Representative The Ohio State University Research Center 1314 Kinnear Road Columbus, OH 43212-1194	2
Director Naval Research Laboratory ATTN: Code 2627 Washington, DC 20375	7
Defense Technical Information Center Bldg. 5, Cameron Station Alexandria, VA 22314	14